

INCREASED STABILITY AND ACTIVITY OF ALCOHOL OXIDASE UNDER HIGH
HYDROSTATIC PRESSURE

by

MARTINA IRENE BUCHHOLZ

(Under the Direction of José Reyes-De-Corcuera)

ABSTRACT

Alcohol oxidase (AOX), in the presence of oxygen, catalyzes the bioconversion of short-chained alcohols into their corresponding aldehydes and ketones. This enzyme has been used for electrochemical biosensors with applications in the food, medical, forensic and environmental industries. Alcohol oxidase has the potential to produce aldehydes that can serve as precursors of fine chemicals and flavour compounds naturally. However due to AOX's poor stability, its practicality for biosensors is very limited. The application of high hydrostatic pressure (HHP) to stabilize and increase the activity of AOX at selected temperatures is reported. Intrinsic thermolabile and thermoresistant fractions of AOX were observed during thermal inactivation at atmospheric and high pressures. The slowest rates of inactivation were generally concentrated between 120 MPa and 160 MPa. A 3.2-fold increase in V_{\max} occurred at 160 MPa at 53.2 °C as compared to the AOX activity at 37 °C and atmospheric pressure.

INDEX WORDS: High hydrostatic pressure; Alcohol oxidase; Enzyme kinetics; Stabilization

INCREASED STABILITY AND ACTIVITY OF ALCOHOL OXIDASE UNDER HIGH
HYDROSTATIC PRESSURE

by

MARTINA IRENE BUCHHOLZ

BS, Purdue University, 2011

A Thesis Submitted to the Graduate Faculty of The University of Georgia in Partial Fulfillment
of the Requirements for the Degree

MASTER OF SCIENCE

ATHENS, GEORGIA

2016

© 2016

Martina Irene Buchholz

All Rights Reserved

INCREASED STABILITY AND ACTIVITY OF ALCOHOL OXIDASE UNDER HIGH
HYDROSTATIC PRESSURE

by

MARTINA IRENE BUCHHOLZ

Major Professor: José Reyes-De-Corcuera, PhD
Committee: Ronald B. Pegg, PhD
William L. Kerr, PhD

Electronic Version Approved:

Suzanne Barbour
Dean of the Graduate School
The University of Georgia
August 2016

DEDICATION

To my family for their continual support. To the late J. Peter Clark, if it was not for his persistence and confidence I may have never attended graduate school.

ACKNOWLEDGEMENTS

I would like to thank my advisor Dr. Reyes-De-Corcuera for his continual support, direction, encouragement and mentorship. I would like to thank Dr. Reyes, the University of Georgia Food Science and Technology Department and the USDA-NIFA grant for providing the funding for my research and conferences. Thank you to my committee members, Dr. Kerr and Dr. Pegg for your guidance and enthusiasm for my research project and classwork. Thank you Dr. Garcia for always being more than willing to help and unwavering motivation. Ali, I will forever be indebted to you. From the start of my career at UGA you have gone above and beyond to help and guide me through this project and other classwork. Thank you to my other lab mates, Juan, Daoyaun, Tristan, Luke and Victoria for providing encouragement and cheer in the lab.

I would like to thank my family and friends for their support, compassion and the constant reminder what a gift it is to be provided such a great education. To George, for literally being by my side every step of the way. Lastly, I am thankful for all of the wonderful friends I have made, experiences I have had and knowledge I have gained.

TABLE OF CONTENTS

	Page
ACKNOWLEDGEMENTS	v
LIST OF TABLES	vii
LIST OF FIGURES	ix
CHAPTER	
1 LITERATURE REVIEW	1
Introduction.....	1
Alcohol Oxidase Characteristics.....	2
Application of Alcohol Oxidase for Biosensors	5
Alcohol Oxidase Stabilization and Increased Activity	14
Gap of Knowledge	21
Hypothesis	23
Objectives	23
2 INCREASED STABILITY OF ALCOHOL OXIDASE UNDER HIGH HYDROSTATIC PRESSURE	32
Introduction.....	32
Materials and Methods.....	34
Results and Discussion	38
Conclusions.....	44

3	INCREASED ACTIVITY OF ALCOHOL OXIDASE UNDER HIGH HYDROSTATIC PRESSURE	53
	Introduction.....	53
	Materials and Methods.....	54
	Results and Discussion	57
	Summary	61
4	FINAL COMMENTS	66
	Overview.....	66
	Future Work	67
	REFERENCES	70

LIST OF TABLES

	Page
Table 1.1: Performance comparison of alcohol biosensors based on alcohol oxidase	24
Table 1.2: Substrates and products for alcohol oxidase.....	27
Table 1.3: Alcohol oxidase stabilization techniques.....	28
Table 1.4: Review of enzymes that are stabilized and/or activated by high pressure.	30
Table 2.1: Comparison of the kinetic rates of alcohol oxidase thermal inactivation at 45 °C and 50 °C for first- and second-order models for one-region and first-order model for two- regions at atmospheric pressure at an enzyme concentration of 0.1 unit mL ⁻¹	45
Table 2.2: Pseudo-first order rate of alcohol oxidase inactivation ± standard error determined by the linear regression of residual activity <i>versus</i> process time.....	46
Table 2.3: Effect of temperature on rate of alcohol oxidase thermal inactivation.....	47
Table 2.4: Effect of pressure on rate of alcohol oxidase thermal inactivation.	47
Table 3.1: <i>In-situ</i> V _{max} for alcohol oxidase at 0.1 and 160 MPa determined by the rate of reaction for 1 min.	62
Table 3.3: <i>In-situ</i> V _{max} for alcohol oxidase at 0.1 MPa between 20 to 37 °C.....	62

LIST OF FIGURES

	Page
Figure 1.1: Schematic representation of an enzymatic biosensor.	31
Figure 1.2: Elliptical pressure-temperature diagram with active and inactive enzyme regions. ...	31
Figure 2.1: High hydrostatic pressure equipment schematic.	48
Figure 2.2: Pressure and temperature profiles in high pressure reactor for sample treated at 59.1 °C at 200 MPa for 10 min and pressure and temperature profiles for treatment at 59.1 °C at 200 MPa for 0 min.	48
Figure 2.3: Alcohol oxidase rate of inactivation at atmospheric pressure and 45.0 °C and 50.0 °C at an enzyme concentration of 0.1 unit mL ⁻¹	49
Figure 2.4: Effect of high hydrostatic pressure on residual activity of L region at 52.6 °C for treatment at 0.1 MPa, 40 MPa, 80 MPa, 120 MPa	49
Figure 2.5: Arrhenius plot for AOX thermal inactivation of the L fraction at 40 MPa, 80 MPa, 120 MPa, 160 MPa, 200 MPa.	50
Figure 2.6: Arrhenius plot for AOX thermal inactivation of the R fraction at 40 MPa, 80 MPa, 120 MPa, 160 MPa, 200 MPa.....	50
Figure 2.7: Eyring plot for AOX thermal inactivation of the L fraction at 49.4 °C, 52.6 °C, 55.8 °C, 59.1 °C, open symbols signify a calculated rate constant at 0.1 MPa.	51
Figure 2.8: Eyring plot for AOX thermal inactivation of the R fraction at 49.4 °C, 52.6 °C, 55.8 °C, 59.1 °C, open symbols signify a calculated rate constant at 0.1 MPa.	51

Figure 2.9: A comparison of the rates of AOX inactivation at 80 MPa and 55.8 °C for L fraction at 0.5 unit mL ⁻¹ and R fraction 1.5 unit mL ⁻¹	52
Figure 3.1: Schematic of high pressure processing equipment using an optical cell and spectrophotometer.....	63
Figure 3.2: Activity displayed as change of absorbance for alcohol oxidase at 0.1 MPa and selected temperatures 37.0, 40.9, 44.9, 49.0, 53.2 °C.....	63
Figure 3.3: Activity displayed as change of absorbance for alcohol oxidase at 160 MPa and selected temperatures 37.0, 40.9, 44.9, 49.0, 53.2 °C.....	64
Figure 3.4: Arrhenius plot for activation energy of alcohol oxidase at 0.1 MPa between 20 to 37 °C (displayed as 10 ³ K).....	64
Figure 3.5: Arrhenius plot for AOX between 37 °C to 53.2 °C (displayed as 10 ³ K) at 0.1 MPa and 160 MPa	65

CHAPTER 1

LITERATURE REVIEW

Introduction

Alcohol oxidase (AOX) in the presence of oxygen catalyzes the bioconversion of short-chained alcohols into hydrogen peroxide and their corresponding aroma active aldehydes and ketones. Alcohol oxidase is a homooctameric flavoprotein, produced by methylotrophic microorganisms. Due to this enzyme's innate qualities, electrochemical biosensors used for the quantitative analysis of alcohol can be produced with AOX.

Alternative alcohol measurements lack the speed and cost efficiency needed for quality assurance in the food industry. Current alcohol biosensors, developed with AOX or alcohol dehydrogenase (ADH), can produce quantitative results swiftly. For this work, AOX will be the main focus. Table 1.1 reviews existing AOX biosensors with descriptions of their characteristics, such as storage and operational stability. Unfortunately, these alcohol biosensors have inadequate longevity because of poor AOX stability. This results in a disadvantageous tool with limited practical application in food processing.

In addition to AOX's potential for biosensors, valuable aldehyde and ketones for industrial use can be produced by AOX initiated reactions (Goodrich et al., 1998). The rate at which AOX catalyzes reactions can be influenced by temperature, concentration, pH, substrate and solvent. While, these manipulations can be beneficial for the rate of reaction, further advancements which increase the production of profitable chemicals could make AOX mediated bioprocesses a desirable method.

This chapter provides background knowledge of AOX activity, stability, and stabilization within the context of fabrication of biosensors and bioprocessing.

Alcohol Oxidase Characteristics

Alcohol oxidase is a homooctameric flavoprotein with a high molecular weight of 600 – 675 kDa (Couderc and Baratti, 1980). Flavin adenine dinucleotide (FAD) is a cofactor bound to each of the eight subunits of AOX. The metabolism of methylotrophic yeasts relies heavily on AOX which is found primarily in the yeast's peroxisomes (Azevedo et al., 2005). The AOX monomers are synthesized on nonmembrane-bound polysomes, then enter the yeasts peroxisomes post-translationally where final AOX assembly is completed (Goodman et al., 1984). Methylotrophic yeast genera's include *Pichia*, *Hansenula*, *Kuraishia*, *Ogataea* and *Candida* (Limtong et al., 2008). The highest substrate affinity AOX has is for methanol with decreasing affinity for increasing chain lengths. For secondary alcohols, which are oxidized into ketones, the affinity is greatly reduced compared to the corresponding primary alcohol (Couderc and Baratti, 1980). The presence of oxygen is required for the reaction acting as the electron receptor.

The optimum temperature for AOX from *Pichia pastoris* is 37 °C and *Hansenula polymorpha*. 45 °C (Couderc and Baratti, 1980). Optimum pH for AOX from *Pichia pastoris* is 7.5 and *Hansenula polymorpha* 8.5 (Couderc and Baratti, 1980). Kato et al. (1976) reported the activation energy (E_a) of *Hansenula capsulata* as 25 kcal mol⁻¹ as compared to Couderc and Baratti (1980) at 45 kcal mol⁻¹ for *Hansenula polymorpha* and 46 kcal mol⁻¹ for *Pichia pastoris*.

Stability of AOX greatly depends on the environment and genera of yeast in which it was produced. Lopez-Gallego et al. (2007) described the inactivation progression of AOX at 45 °C and pH 7 in 10 mM sodium phosphate buffer for *Hansenula sp.*, *Pichia pastoris* and *Candida*

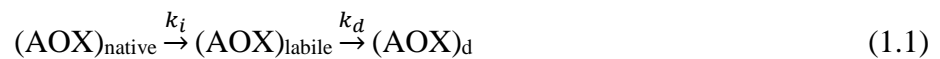
boidinii. *Hansenula sp.* was 1.8 and 4-fold more stable to thermal inactivation than *Pichia pastoris* and *Candida boidinii*, respectively. Lopez-Gallego et al. (2007) concluded that an increase in enzyme concentration (0.01 mg mL⁻¹ to 0.1 mg mL⁻¹) strongly impacted the rate of thermal stability of AOX from *Hansenula sp.* and *Pichia pastoris* at 37 °C and pH 7 in 10 mM sodium phosphate buffer. With the higher enzyme concentration being more stable it was suggested that dissociation of the subunits could be the first step of AOX inactivation. In contrast, Azevedo et al. (2004b) evaluated the thermal stability of *Hansenula polymorpha* at 50 °C in 100 mM phosphate buffer at pH 7 and determined that enzyme concentration (0.025 mg mL⁻¹ and 0.25 mg mL⁻¹) did not impact the stability.

In addition, to reiterating the importance of pH for the thermal stability of AOX from *Hansenula polymorpha*, Azevedo et al. (2004b) concluded that the type of buffer can impact thermal stability. After 8 hours at 50 °C the relative activity of AOX from *Hansenula polymorpha* was 79.0% at pH 7.5, as compared to 64.2% at pH 7.0 and 7.5 % at pH 6.0 in the same 0.1 M phosphate buffer. Illustrating the impact buffers can have on AOX, the residual activity for 0.1 M sodium 3-(*N*-morpholino)propanesulfonate (MOPS) was 37.6% as compared to 64.2% for 0.1 M phosphate buffer at pH 7.0 after 8 hours at 50 °C. Interestingly, the initial activity of AOX for pH 7.0 and 0.1 M MOPS buffer and 0.1 M phosphate buffer were similar with 14.8 ± 0.6 and 14.7 ± 0.5 unit mg⁻¹, respectively.

Alcohol oxidase has been described to show a two-region manner of inactivation (Azevedo et al., 2004b). In other words, instead of fitting a first or second-order rate of inactivation to one linear slope, there are two linear regions of inactivation with different rates. The first being a faster rate, with the second being a slower rate of inactivation. One explanation is that the enzyme is actually a mixture of at least two isoenzymes with different heat

sensitivities, known as parallel models or concomitant models of enzyme thermal inactivation (Aymard and Belarbi, 2000; Greco and Gianfreda, 1984). Dienys et al. (2003) hypothesized two isozymes were present in the AOX they isolated from *Pichia pastoris* based on a wide optimum pH with two maxima. However, a non-denaturing gel electrophoresis presented only one band of AOX, not confirming their hypothesis.

Another two-step deactivation process, known as the series model, was described as the native enzyme degrading to a still active intermediate structure, which eventually will fully inactivate (Greco and Gianfreda, 1984). Azevedo et al. (2004b) hypothesized the stable homooctamer of AOX is quickly converted during thermal inactivation to a more labile yet still active intermediate form, which eventually denatures completely. Equation 1.1 illustrates AOX's hypothesized behavior during thermal inactivation, where k_i and k_d are first order rate constants and $(\text{AOX})_{\text{native}}$ is the native enzyme, $(\text{AOX})_{\text{labile}}$ is the labile intermediate, $(\text{AOX})_{\text{d}}$ is the deactivated enzyme (Azevedo et al., 2004b).



Labile refers to something which is easily broken down, which is misleading because the intermediate form of AOX is more stable to thermal inactivation than the native form. For future work, the “labile intermediate” will be interpreted as the “active intermediate.” For example, AOX from *Hansenula polymorpha* rates of thermal inactivation were fitted to a two-region thermal inactivation model at 50 °C and 0.1 M phosphate buffer at pH 7.5 (Azevedo et al., 2004b). The initial rate, k_i , was $3.3 \times 10^{-2} \text{ min}^{-1}$ which is the initial and faster rate of inactivation.

The second region's rate, k_d , was $7.2 \times 10^{-4} \text{ min}^{-1}$ being the slower rate of inactivation proving that the intermediate form was more stable to thermal inactivation, the opposite of labile. The two-region model provided a better fit with a correlation coefficient of 0.997 as compared to the one-region model with a correlation coefficient of 0.932 and k_d was $4.7 \times 10^{-4} \text{ min}^{-1}$. Verifying the need for a two-region model for AOX during thermal inactivation.

Important to know, AOX has the ability to re-assemble after dissociation. Evers et al. (1995) used 80% glycerol to disassociate AOX into FAD containing monomers. Re-assembly was shown on a non-denaturing PAGE to be most effective at a 5 to 10-fold dilution of the glycerol treated enzyme in 10 mM potassium phosphate buffer with a 30-minute incubation time on ice. The highest reactivation (as compared to untreated AOX) for *Hansenula polymorpha* was ~70% at a 10-fold dilution whereas ~35% for *Pichia pastoris* at a 6-fold dilution. Intriguingly, an active re-assembled hybrid of *Hansenula polymorpha* and *Pichia pastoris* AOX oligomers was achieved. When FAD was removed from native AOX with potassium cyanide prior to dissociation with glycerol, re-assembly was prevented, even with the addition of FAD, demonstrating the vital need AOX has for FAD.

Application of Alcohol Oxidase for Biosensors

Alternative Existing Methods for Alcohol Measurement

For the food industry, specifically the, beverage and alcohol industries, there is a need to detect and quantify alcohol with high sensitivity, selectivity, and speed. Alcohol measurement is needed for on-line control and for post-processing quality assurance of fermentation processes. The quantification of ethanol, produced by fermentation, is necessary for regulatory purposes for stored fruit pulps (Nunes et al., 2016). Furthermore, the amount of alcohol content is important for excise tax purposes for alcoholic beverages (Boujtita et al., 2000). Correct quantification of

alcohol, primarily ethanol, is also very important for medical and forensic applications such as analysis of human breath and blood (Patel et al., 2001). As Personna et al. (2013) described, feasible quantification methods are also needed for onsite environmental analysis of transportation accidents involving ethanol consumption.

Multiple techniques are used to determine the amount of alcohol in a product. The AOAC International Official Methods of Analysis (2012) provides approved methods for the measurement of ethanol and other alcohols in alcoholic and non-alcoholic beverages, including gas chromatography, liquid chromatography, gravimetric techniques, dichromate oxidation, or measurements based on light refraction, and spectroscopy.

The aforementioned techniques for alcohol measurement each have their benefits and downsides. These tests can be reliable and precise, but preparation of the samples can be time prohibitive and complex. When determining the alcohol percentage for alcoholic beverages many techniques begin with distillation or microdistillation to determine the amount of ethanol present: including specific gravity measurements using a pycnometer or a hydrometer, refraction and chemical oxidation (Ough and Amerine, 1988). Several tests require expensive equipment and trained operators such as gas chromatography and liquid chromatography. Azevedo et al. (2005) described how enzymes and their reactions can be used for chemical analysis measured by spectroscopic or electrochemical methods due to the specificity of the target analyte and inherent speed of catalytic activity. For example, Wen et al. (2007) developed an alcohol oxidase biosensor with a one minute response time, which was comparable to similar biosensors with one to two minute response times.

Alcohol Biosensor Characteristics

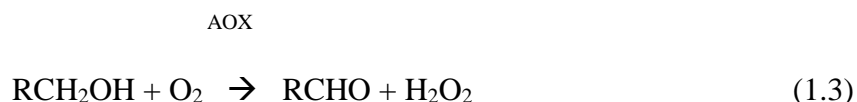
Enzymatic reactions have the potential to produce and/or consume electroactive species which can be measured by electrochemical biosensors. Figure 1.1 provides a fundamental diagram of an enzymatic biosensor. An immobilized enzyme catalyzes an enzymatic reaction with the analyte of interest yielding a response that is converted by an electrochemical transducer into a detectable signal that quantifies the analyte and is displayed on a digital device (Reyes-De-Corcuera, 2015). The two main types of electrochemical transducers for biosensors are potentiometric and amperometric (Reyes-De-Corcuera, 2015; Terry et al., 2005). Potentiometric biosensors measure the difference of potential between a working electrode and a reference electrode. Amperometric biosensors measure current by the electrode oxidation or reduction of an electroactive species produced by the enzyme. This current is proportional to the concentration of analyte present (Terry et al., 2005).

Both amperometric and potentiometric electrochemical biosensors are used to measure alcohol content with alcohol dehydrogenase (ADH) or AOX immobilized on the working electrode. Equation 1.2 displays how nicotinamide adenine dinucleotide (NAD^+) is required as a cofactor in order for ADH to catalyze, the oxidation of primary aliphatic and aromatic alcohols to their corresponding aldehydes (Azevedo et al., 2005). Oxidation of NADH at the surface of a metal electrode of the biosensor is used to obtain the amperometric response and reduce NADH back to NAD^+ (Park et al., 1999).



ADH biosensors for the detection of ethanol have been reported to be more stable and specific than their AOX counterparts (Azevedo et al., 2005). However, AOX biosensors can be preferred because they do not need the addition of NAD^+ . Therefore, AOX and AOX biosensors will be the focus of this research.

Alcohol oxidase catalyzes the oxidation of methanol and other short chained primary alcohols to their corresponding aldehyde (Equation 1.3). Alcohol oxidase biosensors can measure amperometrically or potentiometrically the decrease in O_2 or the increase in H_2O_2 concentration.



Oxygen based measurements have little electrochemical interferences but have low response, reduced accuracy and reproducibility, high background signals causing high detection limits, thus measurements based on H_2O_2 are frequently used to prevent these hurdles. Optical and spectroscopic detection principles may also be used (Azevedo et al., 2005).

Alcohol Oxidase Biosensor Stability and Enhancement

When considering the efficiency of an enzymatic biosensor, storage stability, operational stability, linear range, detection limit, sensitivity and reproducibility need to be considered. Azevedo et al. (2005) and Wen et al. (2007) have previously reviewed the characteristics of published alcohol biosensors based on AOX, as well as the efficiency of non-enzymatic techniques for the quantification of alcohol. Azevedo et al. (2005) stated overall co-immobilized biosensors with AOX and horseradish peroxidase (POD) that had either direct or mediated electron transfer were favorable. Wen et al. (2007) promoted their AOX/chitosan immobilized

eggshell membrane alcohol biosensor as a simple, fast and cost-effective method. Even though their alcohol biosensor had less sensitivity, higher relative standard deviation for reproducibility, and equivalent short-term stability to other reported AOX biosensors. A literature search was conducted on Web of Science on May 15th, 2016 with the search terms *alcohol oxidase biosensor* and “*alcohol oxidase*” AND “*biosensor*” between 2007 and 2016. From 260 hits, 53 journal articles were decided to be relevant. Articles which focused on biosensors developed with other enzymes or made to measure analytes other than alcohols were removed. Table 1.1 provides a review of prominent alcohol biosensors based on AOX since 2007 and onwards.

Chinnadayyala et al. (2014) entrapped the mediator ferrocene with AOX and immobilized it with a sol-gel chitosan film coated with horseradish peroxidase onto a multi-walled carbon nanotube modified glassy carbon electrode producing a biosensor with a low alcohol detection limit of 2.3 μM . This biosensor maintained 90% of the original activity after 28 successive measurements completed in a 5 h period and storage stability of 10% loss of original activity after 4 weeks at 4 °C. The next year Chinnadayyala et al. (2015) produced a biosensor with polyaniline encapsulated gold nanoparticles conjugated with AOX by chitosan-Nafion onto a glassy carbon electrode. This biosensor had a slightly higher detection limit of 7 μM . The operational and storage stabilities were comparable with 6.3% loss of original activity after 25 measurements in a 5 h period and 7% loss of original activity after 5 weeks of storage at 4 °C.

A novel dual biosensor for the quantitative distinction between ethanol and methanol was created (Bucur et al., 2008). The bi-enzymatic biosensor used ADH from *Saccharomyces cerevisiae* to be selective for ethanol while AOX from *Pichia pastoris* measured both ethanol

and methanol. The innovative system had an operational stability of 10 successive measurements with a linear range for the ADH of 0.3 - 8 mM for ethanol and for AOX 3 - 70 mM for methanol and 15 - 110 mM for ethanol.

AOX biosensors need to improve their stability and lower operational costs. Lowering operational costs can be accomplished by reducing the amount of enzyme needed and increasing AOX biosensor reusage capacity. Clearly studies continue to be performed in the lab to develop more efficient biosensors. However, two problems remain. First, as Table 1.1 depicts, there is a lack of standardization for quantification of important biosensor characteristics. Such as, operational and storage stability. Each study assesses their biosensor with a different method, ranging from frequency of use to duration of tests. Sensitivity is also not reported in consistent units. For electrochemical biosensors it should be expressed in units of current density per analyte concentration. However, often current densities are not reported leaving it to the reader to calculate it using the area of electrode. Sometimes this is impossible because the area of the electrodes testing area is not reported. Without standardization in quality measurements, especially in terms of stability, difficulty will persist as to what new methods and technologies are truly the most beneficial in terms of a commercially effective biosensor.

Second, even though research continues for alcohol biosensors, there is limited commercially available alcohol biosensors on the market. The 2900 Series ethanol biosensor from YSI is produced with alcohol oxidase. Unfortunately, the typical working life for this biosensor is 5 days. The detection range for the ethanol biosensor is 0.9 mM to 69.5 mM (Xylem, 2015). Pinnacle Technology Inc. produces a fascinating ethanol biosensor. The biosensor is an implant that performs real-time measurements of ethanol *in vivo* of the brains of rodents for a lifetime of 6 to 8 h. The limit of detection is 0.1 to 0.5 μM and a linear range of at

least 25 mM (Pinnacle, 2012). In 2016 the National Institute on Alcohol Abuse and Alcoholism sponsored a government competition for the challengers to develop “a discreet device capable of measuring blood alcohol levels in near real time.” BACtrack Skyn took home the \$200,000 first place prize for developing a wearable (looks like a watch), non-invasive and low cost alcohol monitoring electrochemical biosensor (BACtrack, 2016). Their proprietary algorithm measures the transdermal alcohol content and proceeds to forward the results via Bluetooth to an iOS device. This incredible device can be set to vibrate the owner’s phone when their blood alcohol content approaches a specific percent. Information was not provided on the source of the biological component or longevity on the biosensor. Fermentations may take days to weeks to complete. For example, wine fermentations vary from 4 to 20 days in length (Tomasi et al., 2013). The goal would be to develop an alcohol biosensor that can continually measure a batch fermentation process, without the need to be calibrated multiple times a day.

Application of Alcohol Oxidase for Bioprocesses

Alcohol oxidase has the potential to naturally produce expensive flavor aldehydes and industrial used chemicals (Goodrich et al., 1998; Murray and Duff, 1990). A review of methods and reusage capabilities (when supplied) for AOX mediated biocatalysis of valued products such as benzaldehyde and glycolaldehyde is provided.

The use of free *versus* immobilized *Pichia pastoris* cells for conversion of ethanol to acetaldehyde was explored by (Duff and Murray, 1988). It was discovered that while conversion rates were lower for immobilized cells, $V_{\max} = 3.17 \text{ g L}^{-1} \text{ h}^{-1}$, compared to the free cells, $V_{\max} = 7.81 \text{ g L}^{-1} \text{ h}^{-1}$, the stability of immobilized cells by calcium alginate increased the temperature stability and reuse capability compared to the free cells by 6-fold at 45 °C. Repeated batch conversion reactions were greatly improved by the immobilized cells. At 30 °C the second batch

cycle lost 18% of the immobilized cell's activity as compared to the free cells at 60%, and for the third batch cycle a loss of 33% for the immobilized cells as compared to the free cells activity loss at 90%. (Duff and Murray, 1988).

Although Fujii and Tonomura (1972) discovered that AOX from *Candida* N-16 could oxidize benzyl alcohol to benzaldehyde, Duff and Murray (1989) used a two phase organic/aqueous system and three versions of AOX to produce far greater amounts of benzaldehyde. The three versions included whole cells of *Pichia pastoris*, isolated AOX from *Pichia pastoris* and the isolated AOX immobilized onto a diethylaminoethyl (DEAE) Biogel. Benzyl alcohol and benzaldehyde have low water solubilities and the potential to inhibit AOX. Dependent on the organic solvent chosen, the two phase system enhances the solubility of the reactant and product, while limiting high concentrations of the compounds which inhibit AOX. With only 10% loss in enzymatic activity, immobilization was said to stabilize AOX. However quantification of stabilization was not reported (Duff and Murray, 1989). This lab went on to discover the capability of *Pichia pastoris* whole cells to bio-oxidize other aliphatic and aromatic high molecular weight alcohols (hexanol, octanol, nonanol, decanol, undecanol, phenethyl alcohol, 3-phenyl-1-propanol) using biphasic reaction medium consisting of 3% water and 97% (v/v) water-saturated hexane (Murray and Duff, 1990).

Pichia pastoris whole cells were used to oxidize alcohols in orange water phase essence or orange aroma with the general objective to improve quality and value by increasing the acetaldehyde content (Goodrich et al., 1998). A whole cell system was used at 30 °C instead of isolated AOX because of the endogenous benefits of cofactor regeneration and additional enzyme systems, such as formaldehyde dehydrogenase (Goodrich et al., 1998). The model system with *Pichia pastoris* cells generated acetaldehyde, propanal and octanal from the orange

aroma. Sensory tests of the modified orange aroma rated higher by a trained panel for orange character, freshness and fruitiness attributes.

Isobe and Nishise (1995) determined the optimum reaction conditions for production of glycolaldehyde from ethylene glycol by AOX from *Pichia pastoris*. A raw material, glycolaldehyde is used to synthesize serines, tryptophan, agrochemicals and medicines (Isobe and Nishise, 1995; Ukeda et al., 1998). Chemical methods of production have limitations including low conversion yields, high concentration of by-products and very high, 500 – 600 °C, reaction temperatures (Majerski et al., 2006; Ukeda et al., 1998). Since AOX can also oxidize glycolaldehyde to glyoxal, Isobe and Nishise (1995) demonstrated the need of a high ethylene glycol concentration, 2 to 6 M, to produce glycolaldehyde, while inhibiting the production of glyoxal. The optimum conditions for producing glycolaldehyde are incubating less than 1 M ethylene glycol with 50 units of AOX *Pichia pastoris*, in 0.8 M Tris-HCL, pH 9.0, with 2600 units of catalase at 5 °C (Isobe and Nishise, 1995). Three years later Ukeda et al. (1998) improved the technique using immobilized AOX and catalase. The optimum conditions for this method included immobilizing AOX from *Pichia pastoris* and catalase from *Aspergillus niger* onto Chitoparl BCW 3501 in 1.5 M Tris-HCL buffer and pH 9.0 at 2 °C. Under these conditions 0.97 M glycolaldehyde was produced from 1.0 M ethylene glycol with a ratio of glyoxal to glycolaldehyde less than 1%. Also, under these conditions the repetitive use was tested and the production rate did not significantly change after 6 repeated uses for a total of 250 h (Ukeda et al., 1998).

Isobe et al. (2012) reviewed the oxidation of glycolaldehyde into glyoxal by microbial oxidases. Sources including the methylotrophic yeasts *Candida* sp. and *Pichia pastoris* and from fungal strains *Aspergillus ochraceus* and *Penicillium purpurescens*. Intriguingly, a novel AOX

from *Paenibacillus* spp. AIU 311, reported high activity for aldehyde alcohols, such as glycolaldehyde and glyceraldehyde, but not short-chained primary and secondary alcohols (Isobe et al., 2007). Glyoxal, a multipurpose organic chemical, formation has similar disadvantages to glycolaldehyde production, thus improving current known enzymatic reactions for production should be investigated.

Table 1.2 displays the wide breadth of substrates AOX has the ability to oxidize into their respective products. Columns 4 to 6 describe the rate of methanol oxidized by AOX to be 100% rate of oxidation. The other substrates rate of oxidation is then compared to methanol's rate of oxidation. The large array of substrates for AOX could provide for argument that AOX is not selective enough to produce an effective ethanol biosensor. The assumption can be made that the samples would not contain an interfering amount of the other substrates and because of their rates of oxidation it should not be a problem.

Alcohol Oxidase Stabilization and Increased Activity

Multiple methods and combinations of such methods are utilized to enhance the stability or activity of enzymes. As stated by Eisenmenger & Reyes-De-Corcuera (2009a) genetic engineering and/or immobilization of the enzyme and operating in non-aqueous media are stabilization techniques. Immobilization of the enzyme(s) onto the electrode restricts the enzyme(s) to a distinct area, allowing for repeated and continuous use of their catalytic properties (Katchalski-Katzir, 1993). The technique for immobilization of AOX can have a great impact on the quality and longevity of the biosensor. Techniques for immobilizing AOX onto the surface of an electrode range from trapping AOX into polymeric films or between membranes, adsorption, crosslinking and covalent tethering (Reyes-De-Corcuera, 2015).

Dissociation of subunits is a limitation for successfully stabilizing multimeric enzymes, like AOX, because of the difficulty attaching all subunits to a planar surface. In order to further stabilize the quaternary structure of such complex proteins, multifunctional reagents have been used to further crosslink the enzyme to whatever structure it is immobilized to (Betancor et al., 2003). Table 1.3 reviews a variety of stabilization techniques for AOX showing the method, most stable version and the measured stabilization increase. Azevedo et al. (2004b) and Gibson et al. (1993) explored the use of sugars, sugar alcohols, and polymers for enzymatic stabilization with much success. For example, 0.1% dextran sulphate used in conjunction with 50 mM lactose maintained 99.9% of AOX activity after 9 h at 50 °C as compared to 54% without stabilizer.

Lopez-Gallego et al. (2007) determined the most stable support for AOX from *Pichia pastoris* to be covalent immobilization with glyoxyl agarose and for AOX from *Hansenula sp.* ionic adsorption on agarose coated with polyethylenimine (PEI). Other less stable supports studied included monoaminoethyl-*N*-ethyl-agarose, glutaraldehyde agarose and amino epoxide-sepabeads. Glyoxyl agarose was unable to attach all of the enzyme subunits. Dextran aldehyde added to the glyoxyl-AOX derivatives was used to crosslink the unattached subunits as a post-immobilization technique to prevent enzyme dissociation. Even though this provided stability, the activity was below 20% for the dextran aldehyde adjusted glyoxyl agarose support. The PEI coated supports exhibited high activity, greater than 50%, for both enzymes. The polymeric bed produced by the PEI-coated supports were described to have a volume that permitted multi-subunit interaction.

A common theme of AOX stabilization is the use of multiple methods. As novel AOX immobilization methods continue to improve and increase stabilization, advanced fine-tuning for increased activity, substrate selectivity and multi-enzyme reaction is possible

High Hydrostatic Pressure Enzyme Stabilization

A possible novel technique for biosensor stabilization is using high hydrostatic pressure (HHP) processing to stabilize the enzyme of interest in combination with immobilization. In 1914, a Harvard physics professor, Percy W. Bridgman, discovered that egg albumin appeared to coagulate in the presence of high pressure at room temperature (Bridgman, 1914). Throughout the 1900's research continued to utilize high pressure processing for the advancement of biosciences. Originally used as a non-thermal processing technique to inactivate damaging enzymes and harmful microorganisms, the use of HHP processing has expanded in the food industry. At varying pressure-temperature treatments, HHP has shown the capability to stabilize and increase the activity of many enzymes.

Eisenmenger and Reyes-De-Corcuera (2009b) provided a thorough review of enzymes that are enhanced with HHP by stabilization and/or an increase in activity. An array of hydrolases, transferases, oxidoreductases and one lyase were discussed. For example, an unidentified protease from *Methanococcus jannashii* had 3.4-fold increase in reaction rate and 2.7-fold increase in thermostability at the high temperature of 125 °C and 50 MPa (Michels and Clark, 1997). Displaying the wide range of pressures and temperatures which enzymes are most active and/or stabilized polyphenoloxidase (PPO) from red raspberry increased activity by 8% at the high pressure of 800 MPa at a temperature of 18 – 22 °C (Garcia-Palazon et al., 2004).

Recent (2009 to present) studies of oxidoreductases under HHP are summarized in Table 1.4. Alcohol dehydrogenase's behavior under HHP is also reviewed in Table 1.4 as well as the aforementioned enzymes under HHP from the Eisenmenger and Reyes-De-Corcuera (2009b) review article.

Polyphenoloxidase has exhibited a wide range of pressure stability, with the primary factor being origin, with other impactful factors such as pH and presence of salt (Buckow et al., 2009). Investigation into the inactivation kinetics for PPO from Boskop apples discovered that pressures below 300 MPa had an antagonistic effect with temperature, requiring temperature to be increased 10 to 15 °C at 100 to 300 MPa in order to inactivate the PPO (Buckow et al., 2009). Terefe et al. (2010) attempted to inactivate PPO from strawberry puree, cultivar Aroma, at 100 to 690 MPa and 24 to 90 °C for 15 min without significant success. While increase in stability was not specifically reported, residual activity was greater than 100% for multiple pressure-temperature-time domains; including 100 MPa at 90 °C for 15 min at 105.3%, 395 MPa at 57 °C for 15 min at 108.9%, 690 MPa at 24 °C for 5 and 15 min at 116.1% and 112.5%, respectively. Peroxidase from strawberry puree, cultivar Aroma was less stable to temperature and pressure. At pressures 100 to 400 MPa, POD was slightly stabilized by HHP against thermal denaturation, a precise amount of stabilization was not reported. Notably, Terefe et al. (2010) discussed and observed the two regions when determining the rate of inactivation for POD under thermal inactivation.

Dallet and Legoy (1996) studied the conformational and catalytic changes induced by HHP on yeast ADH and ADH from *Thermoanaerobium brockii* (TBADH). The ADH from yeast, a mesostable tetrameric enzyme, was inhibited by an increase in pressure. The TBADH, a thermostable tetrameric enzyme, was determined to have enhanced activity up to 200 MPa with a maximum at 100 MPa at 40 °C. Subunit dissociation was not attributed as the cause for thermal inactivation for either enzyme, rather a molecular rearrangement. Because the thermostable ADH was more thermostable than the mesostable ADH, it was suggested that thermostability and barostability were linked. Using a dimeric ADH from horse liver, V_{\max} was determined to be 10-

fold higher than at 200 MPa at 30 °C and pH 8 as compared to 0.1 MPa under same conditions (Trovaslet et al., 2003). Further investigation with Fourier transform infrared spectroscopy determined that the denaturation of ADH from horse liver under pressure was a multi-step process. Pressure up to 400 MPa did not induce subunit dissociation of the ADH from horse liver. Molten globule like states were observed at 400 MPa and 600 MPa and explained to be two independent structural domains with different HHP stability, a coenzyme binding domain and a catalytic domain (Trovaslet et al., 2003; Trovaslet et al., 2004). Undoubtedly, optimal conditions for stabilization and activation of enzymes cover a large range of temperatures, pressures, substrates, pH and solvents.

Multiple mechanisms are thought to contribute to pressure-induced stabilization of enzymes against thermal inactivation. Increased pressure and temperature produce opposing effects for an enzyme. Unlike high temperature, HHP increases the hydration of enzyme's charged and non-polar groups hampering water loss (Mozhaev et al., 1996). Loss of water from the protein shell has been hypothesized as an initial step of thermal inactivation (Boonyaratanakornkit et al., 2002). While heat disrupts hydrogen bonds, HHP has been thought to enhance and promote formation of hydrogen bonds (Eisenmenger and Reyes-De-Corcuera, 2009b). In contrast, increased temperatures (60 to 70 °C) reinforces hydrophobic interactions but are weakened by pressure increase (Bilbao-Sáinz et al., 2009; Eisenmenger and Reyes-De-Corcuera, 2009a). Splitting of the secondary structure's hydrogen bonds, due to either very HHP or high heat, leads to irreversible denaturation of an enzyme (Hendrickx et al., 1998). Hawley (1971) utilized an elliptical diagram (Figure 1.2) to illustrate the relationship between pressure and temperature effects on enzyme conformation. With the native/active protein represented inside and the denatured/inactive conformation on the outside, separated by a darker region

symbolizing reversible denaturation. The pressure at which stabilization and inactivation by HHP occurs is dependent on the particular enzyme and surrounding environment and currently determined experimentally.

Presently, empirical models must be built based on experimentation because no mathematical model established by the molecular structure of enzymes can predict how each enzyme behaves at HHP. To date, there has been no published work on the behavior of AOX at HHP. Application of the presumptive HHP-stabilized AOX offers an opportunity to build biosensors with increased longevity. In other words, immobilizing AOX at the optimal HHP onto the working electrode of alcohol biosensors could capture the protein's stabilized form. The assumption can then be made that the alcohol biosensor would have an increased operational and storage stability as a result of the HHP modified enzyme.

Enzymatic stabilization by HHP for biosensors is a technique that could be used for other food industry applicable enzymatic biosensors. Mello and Kubota (2002) provided a review of biosensors for food analysis. For example, biosensors can quantify analytes such as glucose, fructose, glycerol, polyphenols, ascorbic acid, and sulfite by the enzymatic biocomponents glucose oxidase, D-fructose dehydrogenase, glycerokinase and glycerol-3 phosphate oxidase, ascorbate oxidase, and sulfite oxidase, respectively. Other biosensors include xanthine biosensors made with xanthine oxidase that can detect the freshness of fish (Pundir and Devi, 2014). Or pyruvate oxidase biosensors which can be used to determine phosphate ions in environmental samples or pungency of onions (Abayomi et al., 2006; Yablotskii and Shekhovtsova, 2010)

Increased Activity of Enzymes under High Hydrostatic Pressure

High hydrostatic pressure not only can stabilize enzymes from thermal inactivation, but also can increase the catalytic activity of the enzymes. According to Eisenmenger and Reyes-De-Corcuera (2009b), summarized how pressure prompts reaction rate changes for an enzyme into three groups: 1) direct change of enzyme structure, 2) reaction mechanism changes, 3) solvent or substrate physical property changes that could affect group 1 or 2. Enzymatic activity can be enhanced by a decrease in volume predicted by Le Châtelier's principle. Eyring's equation can be used to predict the effect of pressure on reaction rate. Equation 1.4 is an integrated and rearranged version of Eyring's equation. where the rate constant is k_o , specific pressure is P , absolute temperature is T , R is the ideal gas constant ($8.3145 \text{ J mol}^{-1} \text{ K}^{-1}$), ΔV^\ddagger is the activation volume, k_{P_o} is the rate constant at reference pressure P_o .

$$\ln(k_o) = \left(\frac{\Delta V^\ddagger}{RT} \times P \right) + \ln(k_{P_o}) \quad (1.4)$$

A specific example of increased catalytic activity under HHP is the 6.5-fold increase of α -chymotrypsin with an anilide substrate at 20°C and 470 MPa as compared to 0.1 MPa (Mozhaev et al., 1996). Moreover, with a rise in temperature the increase in catalytic activity under HHP is greater because of activation volume's temperature dependence. At 50°C and 360 MPa , α -chymotrypsin's activity increased 30 times as compared to 20°C at 0.1 MPa (Mozhaev et al., 1996). Eisenmenger and Reyes-De-Corcuera (2009b) provided a comprehensive review of HHP enhanced enzymes of studies performed before 2009. Recently, HHP increased the catalytic activity of a commercial blend pectinase from *Aspergillus niger* and a citrus derived

pectin substrate by 2.3 times under 300 MPa and 62.4 °C as compared to the traditionally used atmospheric pressure and 45 °C (Tomlin et al., 2014). Techniques using AOX to catalyze the production of useful chemicals, could be improved with proof that HHP has the ability to increase the activity of AOX.

Gap of Knowledge

Alcohol oxidase (AOX) biosensors present a rapid and selective instrument for the food and beverage industry. Unfortunately, AOX biosensors lack the stability needed to be an effective commercialized tool. The primary way to increase the longevity of an enzymatic biosensor is to increase the stability of the enzyme. Stabilization methods ranging from chemical modification, crosslinking, and the use of polyelectrolytes have been employed to stabilize AOX.

High hydrostatic pressure (HHP) has been utilized as a technique to stabilize enzymes. Multiple hypothesis attempt to explain how HHP positively affects enzyme stability. The primary conclusion is that temperature and pressure work antagonistically on the molecular level. In other words, increase in temperature increases entropy, while increase in pressure increases order, thus decreases entropy (Eisenmenger and Reyes-De-Corcuera, 2009a). Each enzyme is specific in terms of which pressure-temperature combination provides the most stability. Several gaps of knowledge arise when determining if HHP can be applied as a technique to improve the stability of alcohol biosensors. Primarily, a study needs to be completed to determine if AOX can be stabilized by HHP. Currently, empirical models are made based on experimental results because no mathematical model based on the molecular structure of enzymes can predict how each enzyme behaves at HHP.

Alcohol biosensors are made from two primary sources of AOX *Pichia pastoris* and *Hansenula polymorpha*. Literature has shown for other enzymes, such as polyphenoloxidases,

that different sources of the same enzyme behaves differently at HHP due to native characteristics. Thus experimentation would need to be performed to determine the optimal HHP for AOX obtained from different sources.

Although enzymatic stabilization has been shown, further insight is needed to determine what happens to the stabilized enzyme after depressurization. If loss of stability for the presumptive HHP-stabilized AOX is rapid, techniques would need to be developed to capture the stabilized form onto the working electrode. Building the alcohol biosensor under pressure inside the reactor is an option that should be explore. Furthermore, experiments would have to be performed to conclude if immobilized HHP-stabilized AOX alcohol biosensors improved the stability, sensitivity, reproducibility as compared to current versions of alcohol biosensors.

High hydrostatic pressure has also been shown to increase the activity of enzymes, primarily because temperature of the reaction can be increased, as a result of an HHP-stabilized enzyme. An increase in AOX activity could result in the rapid production of valuable chemicals potentially providing a natural and/or cost effective method. Experimentation is needed to determine if HHP can increase the activity of AOX. Initially, substrates which AOX has a high specificity for, such as methanol and ethanol would be tested. Then substrates which produce valuable chemicals such as benzaldehyde or glycolaldehyde from benzyl alcohol and ethylene glycol, respectively. Lastly, adjustments to the environment other than temperature and pressure can be manipulated, such as pH and solvents, to increase the production of products.

The treatment of enzymes, especially AOX, by HHP has possible applications for the food industry and should be further investigated.

Hypotheses

1. High hydrostatic pressure increases the thermal stability of AOX.

2. High hydrostatic pressure increases the catalytic activity of AOX.

Objectives

This project will focus on the impact HHP can have on AOX. Knowledge gained will be applied to biosensor manufacturing and biocatalytic reactions. Data obtained from the stabilization of AOX at HHP will determine if the technique can be used to produce an alcohol biosensor with increased stability. The kinetic behavior of AOX at HHP will govern if further studies should pursue the technique as an alternative method to produce fine chemicals.

Specific Objectives

1. The aim of the first study is to determine an optimum HHP that best stabilizes AOX at selected temperatures.
2. The aim of the second study is to maximize the catalytic activity of AOX at selected temperatures, in a range of pressures that stabilize the enzyme.

Table 1.1 Performance comparison of alcohol biosensors based on alcohol oxidase.

Immobilization Technique	AOX Source	Working Electrode	Potential Applied	Detection Limit	Linear Range	Sensitivity	Operational Stability	Storage Stability	RSD ^a , %	Reference	Notes
Polyamido-amine dendrimers	<i>P. pastoris</i>	Cysteamine-modified gold electrode	-0.7 V vs. Ag/AgCl	0.016 mM	0.025 to 1.0 mM		2% loss after 8 measurements over 8 h at 25 °C	32% loss after 1 month, with measurements every 2 days, stored at 4 °C	0.2 and 0.5 mM ethanol, 0.8% and 4.9% respectively	Akin et al. (2010)	Applied to both batch and flow injection analysis systems
GA cross-linked AOX in the presence of BSA	<i>H. polymorpha</i>	PNR-mediate carbon film	-0.3V vs. SCE	30 µM	up to 0.7 mM	860 nA/mM cm ²	57.6% sensitivity remained after 3 weeks of 2 to 3x per week use ^c	12% loss after 6 weeks at 4 °C		Barsan and Brett (2008)	Using PNR increased sensitivity by a factor of 5 as compared to without
Entrapment in PVA-SbQ	ADH: <i>S. cerevisiae</i> AOX: <i>P. pastoris</i>	ADH: MB mediated SPE, AOX: CPT mediate SPE	ADH: -10 mV vs. Ag/AgCl	ADH: 0.1 mM EtOH AOX: 10 mM EtOH, 1 mM MeOH	ADH: 0.3 - 8 mM for EtOH AOX: 3 - 70 mM for MeOH, 15 - 110 mM for EtOH		10 successive measurements ^c		ADH: 14 AOX: 16.2 for same lot and 41 for different batches	Bucur et al. (2008)	Novel dual biosensor for distinction between EtOH and MeOH quantities
Ferrocene entrapped AOX and sol-gel CS film coated HRP	<i>P. pastoris</i>	Multi-walled carbon nanotube modified glassy carbon	-0.34V	0.0023 mM	0.005 - 3 mM	150 µA/mM cm ²	10% loss of activity after 28 successive measurements completed in 5 h ^c	90% after 4 weeks at 4 °C	2	Chinnadayya et al. (2014)	Enhanced activity of AOX by entrapment of ferrocene
PA encapsulated AuNP conjugated with AOX by CS-Nafion	<i>P. pastoris</i>	Glassy carbon electrode	+0.6V	7 µM	0.01 - 4.7 mM	348 µA/mM cm ²	93.7% of initial activity after 25 measurements in 5 h ^c	93% after 5 weeks at 4 °C	2.4	Chinnadayya et al. (2015)	The AuNP increased the kinetic activity of AOX

Immobilization Technique	AOX Source	Working Electrode	Potential Applied	Detection Limit	Linear Range	Sensitivity	Operational Stability	Storage Stability	RSD ^a , %	Reference	Notes
GA vapor with 5% BSA	<i>Hansenula sp.</i>	Platinum printed	+200 mV vs. intrinsic reference electrode	0.3 mM	0.3 to 40 mM			140% after 2 months, 20% after 3 months	4.2	Goriushkina et al. (2009)	Glucose oxidase and lactate oxidase biosensors were also developed
GA cross-linked AOX in the presence of BSA	<i>P. pastoris</i>	Graphite pasted SPE coated with Prussian Blue	0V vs. Ag/AgCl	0.09 mM	up to 90 mM	480 nA/mM ^b	2% RSD in 15 successive measurements ^c		10	Kamanin et al. (2015)	Biosensors for the measurement of glucose, lactate and starch were also developed
AOX on PA film	<i>P. pastoris</i>				0.01% - 8%			Up to 7 weeks at 4 °C	1.6	Kuswandi et al. (2014)	Visual biosensor in dip-stick format for halal verification
				0.1 to 0.5 μM	At least 25 mM			6 to 8 h		Pinnacle (2012)	<i>In vivo</i> brain implant for real-time measurement in rodents
AOX with CS on an eggshell membrane	<i>Hansenula sp.</i>	Platinum		30 μM	0.06 - 0.8 mM		No loss after 20 measurements carried out in 8 h, at 20 to 25 °C	86.6% after 3 months, at 3 day intervals and 4 °C	3.4	Wen et al. (2007)	Highlights include cost-effective, simple sensor design and ease of operation

Immobilization Technique	AOX Source	Working Electrode	Potential Applied	Detection Limit	Linear Range	Sensitivity	Operational Stability	Storage Stability	RSD ^a , %	Reference	Notes
AOX and HRP in an ionotropy polymer hydrogel matrix	<i>Hansenula sp.</i>			2.3 mM	2.3 - 90 mM MeOH in <i>n</i> -hexane		82% of original value after 45 assays ^c	60% of original magnitude after 15 days at 4 °C		Wu et al. (2007)	Organic-phase alcohol biosensor to measure methanol in a gasoline sample, optical sensor
		Proprietary ion selective electrode			0.9 mM to 69.5 mM		5 days, 15 to 35 °C			Xylem (2015)	Commercial ized ethanol biosensor

^a Reproducibility of biosensors reported as relative standard deviation, %

^b Area of electrode was not reported

^c Temperature was not reported

ADH = alcohol dehydrogenase, AOX = alcohol oxidase, AuNP = gold nanoparticles, BSA = bovine serum albumin, CPT = co-phthalocyanine, CS = chitosan, EtOH = ethanol, GA = glutaraldehyde, HRP = horseradish peroxidase, MeOH = methanol, PA = polyaniline, PNR = poly(neutral red), PVA-SbQ = polyvinyl alcohol containing stilbazolium groups, RSD = relative standard deviation, SCE = saturated calomel electrode, SPE = screen-printed electrodes, MB = Meldola blue

Table 1.2 Substrates and products for alcohol oxidase.

Substrate	Product	Relative Rate of Oxidation (%)			% substrate oxidized to product
		Patel et al. (1981)	Couderc and Baratti (1980)	Dienys et al. (2003)	
Methanol	Formaldehyde	100	100	100	
Formaldehyde	Formate	15			
Ethanol	Acetaldehyde	92	82	83	
2-Chloroethanol	Chloroacetaldehyde	70		66	
Allyl alcohol	Acrolein			81	
Ethylene glycol	Glycolaldehyde	15		40	
Glycolaldehyde ^a	Glyoxal				
2-Cyanoethanol	Cyanoacetaldehyde			30	
2-Mercaptoethanol	Mercaptoacetaldehyde	25			
1-Propanal	Propionaldehyde	74	43		
2-Propanal	Acetone	0	2		
3-Chloro-1-propanol	2-Chloropropanal	22			
Propargyl Alcohol	Propiolaldehyde			90	
1-Butanol	Butyraldehyde	52	20	67	
Isobutanol	Isobutyraldehyde	2	1.2	21	
2-Butanol	Butanone	0	0.2		
2-Methyl-1-butanol	2-Methylbutanal	22			
4-Chloro-1-butanol	4-Chlorobutanal	11			
1-Pentanol	Pentanal	30			
1-Hexanol	Hexanal	4			41.3
Heptanol	Heptanal				51.5
Benzyl alcohol	Benzaldehyde				
Octanol	Octanal		0		47.5
Phenethyl alcohol	Phenyl acetaldehyde				2 ^b
Nonanol	Nonanal				3.5
3-phenyl-1-propanol	3-Phenylpropanal				54
Decanol	Decanal				3.5
Undecanol	Undecanal				2 ^b
	Reference	Patel et al. (1981)	Couderc and Baratti (1980)	Dienys et al. (2003)	Murray and Duff (1990)

^a V_{\max} reported as 0.46 $\mu\text{mol}/\text{min}/\text{mg}$ of protein by (Isobe et al., 2012)

^b After 72 h as compared to 24 h for the rest in column

Table 1.3 Alcohol oxidase stabilization techniques.

Method of Stabilization	Most Stabilized Version	Measurement of Stability	Notes	Reference
AOX from <i>Hansenula polymorpha</i> immobilized on CPG by covalent attachment using GA as crosslinker	Activating CPG with 6.5% GA for 1 h at pH 7, CPG support with 120 – 200 mesh and 550 Å pore size	Bioreactors operated for more than 14 h at 32 °C with < 5% significant loss of performance	14 in the bioreactor corresponds to an equivalent number of 33,600 injections of 25 µL of 6.5 mM in a FIA	(Azevedo et al., 2004a)
Effect of sugar on AOX from <i>H. polymorpha</i>	50 mM lactose and 10 mM melezitose	< 20% of activity was lost after 9 h at 50 °C as compared to 54% without stabilizer	Other sugars tested included glucose, fructose, lactose, maltose, trehalose	(Azevedo et al., 2004b)
Effect of polymer on AOX from <i>H. polymorpha</i>	0.01% PEG 400	89.1% activity remained after 9 h at 50 °C as compared to 54% without stabilizer	Dextran and PEIs were also evaluated and displayed stabilization to a lesser degree	(Azevedo et al., 2004b)
Effect of polymer and sugar alcohol on AOX from <i>H. polymorpha</i>	0.1% dextran sulphate and 50 mM lactose	99.9% activity remained after 9 h at 50 °C as compared to 54% without stabilizer	15% activity enhancement was also observed	(Azevedo et al., 2004b)
Dried AOX stabilized with sugar alcohols in conjunction with cationic polymer.	Most stabilized with a combination of inositol and DEAE	Retained 80 to 100% of activity over periods up to 2 months at 37 °C, whilst control lost 74% over just 7 days at 37 °C	Other sugar or sugar alcohols tested (lactitol, sucrose, lactose, maltitol) were effective with DEAE to a lesser extent	(Gibson et al., 1993)
Carrier-free CLEA method with AOX from <i>Pichia pastoris</i>	With 67% isopropanol precipitated for 2 h, then crosslinked with 5 mM GA for 24 h	After 12 weeks more than 50% of AOX activity remained at 8 and 22 °C	Method does not require a carrier or a support	(Gruskiene et al., 2015)
AOX immobilized onto magnetic beads prepared with GMA and MMA via polymerization with the crosslinker EGDMA	The 75 to 150 µm size beads	Operational stability was constant for 20 measurements after the first 5 measurements	Activity of the smaller beads (50 to 75 µm) was 4.8-fold higher than the larger beads	(Kiralp et al., 2008)
Covalent immobilization and crosslinking using AOX from <i>Pichia pastoris</i> and <i>Hansenula</i> sp.	Glyoxyl agarose with dextran aldehyde to crosslink the enzyme subunits not attached to the support	“Good stabilization achieved”, numerical value of stabilization not reported	Low activity, < 20%	(Lopez-Gallego et al., 2007)
Ionic adsorption using AOX from <i>Pichia pastoris</i> and <i>Hansenula</i> sp.	Agarose coated with 600 kDa PEI	“Good stabilization achieved”, numerical value of stabilization not reported	Recovered activity was over 50%	(Lopez-Gallego et al., 2007)
GA activated covalent immobilization of AOX from <i>Pichia pastoris</i> onto PEI grafted electrospun PSMA fibers	PSMA-PEI-AOX fibers	After 24 h at 45 °C 75% activity remained as compared to control at 25 °C	Used for color strips to determine ethanol in saliva, temperature optimum shifted to 50 °C from 40 °C	(Zhao et al., 2013)

CLEA = crosslinked enzyme aggregate, CPG = propylamino-derivatised controlled pore glass, DEAE = diethylaminoethyl, EGDMA = ethylenedimethylmethacrylate, FIA = flow injection analysis system, GA = glutaraldehyde, GMA = glycidylmethacrylate, MMA methylmethacrylate, PEG = polyethylene glycols, PEI = polyethylenimine, PSMA = polystyrene-co-maleic anhydride

Table 1.4 Review of enzymes that are stabilized and/or activated by high pressure.

Enzyme (EC class)	Source	Solvent	Pressures Tested (MPa)	Temperatures Tested (°C)	Optimal Conditions	Notes	Reference
Polyphenoloxidase (EC 1.14.18.1)	Boskop apples	Cloudy apple juice	0.1 - 700	20 - 80	20 - 45 °C, 300 MPa	In order to inactivate the PPO, temperature had to be increased 10 – 15 °C at 100 – 300 MPa	(Buckow et al., 2009)
	Strawberry puree, cv. 'Aroma'	Strawberry puree	100 - 690	24 - 90	690 MPa and 24 °C resulted in 16 % increase activity	Inactivation was attempted with the pressure and temperature ranges and little success	(Terefe et al., 2010)
	Red raspberry	Red raspberry	400, 600, 800	18 – 22	400 and 800 MPa	Increased activation by 15 and 8% at 400 and 800 MPa, respectively after 5 min treatment	(Garcia-Palazon et al., 2004)
Peroxidase (EC 1.1.1.x)	Strawberry puree, cv. 'Aroma'	Strawberry puree	100 - 690	24 - 90	100 - 400 MPa	Followed a first-order two region model, indicating stable and labile isoenzymes	(Terefe et al., 2010)
Dehydrogenase (EC 1.1.1.1)	<i>Thermoanaerobium brockii</i>	Tris/HCl, pH 7.8	0 – 200	40	100 MPa	Maximum activity at 100 MPa, activity was enhanced up to 200 MPa	(Dallet and Legoy, 1996)
	Horse liver alcohol dehydrogenase	Tris/HCl, pH 8	0 – 250	30	200 MPa V_{max} was 10x higher compared to 0.1 MPa	A Fourier transform infrared spectroscopy study confirmed 400 MPa did not induce subunit dissociation, but rather a dimeric molten globule at 400 MPa	(Trovasset et al., 2003)
Protease (Unidentified)	<i>Methanococcus jannashii</i>	HEPES, pH 6.5	1, 25, 50	90 – 130	50 MPa and 125 °C	3.4-fold increase in reaction rate and 2.7-fold increase in thermostability at optimal conditions	(Michels and Clark, 1997)

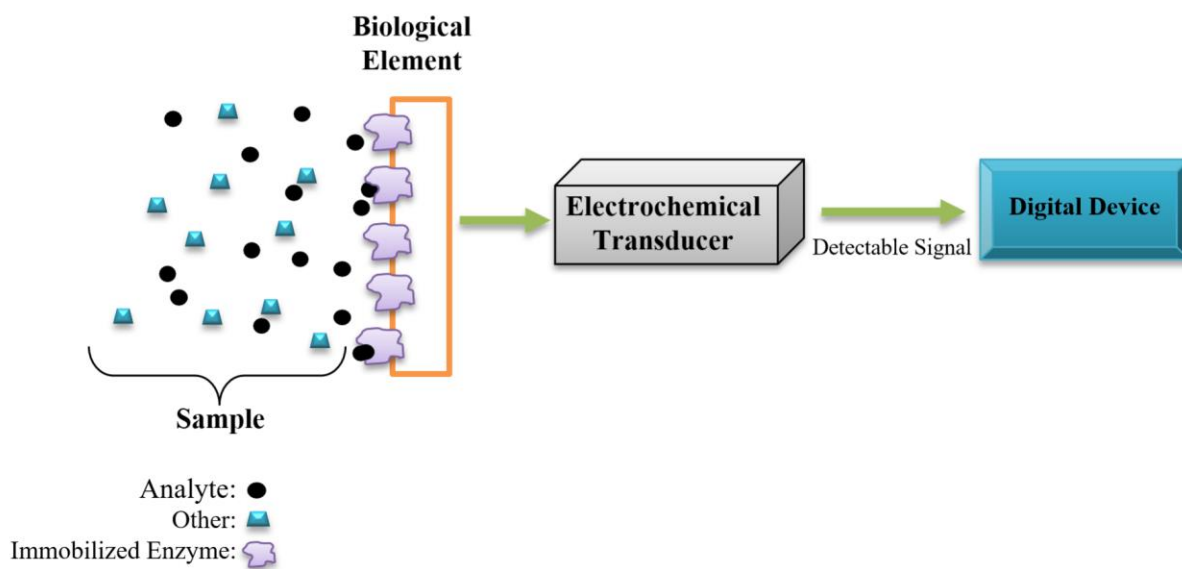


Figure 1.1. Schematic representation of an enzymatic biosensor.

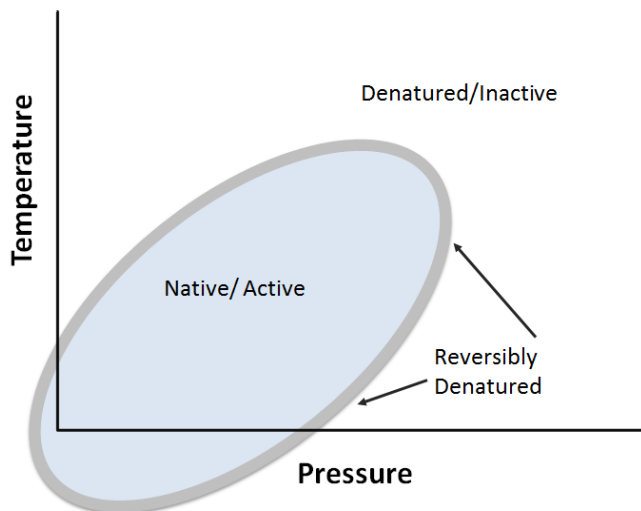


Figure 1.2 Elliptical pressure-temperature diagram with active and inactive enzyme regions.

CHAPTER 2

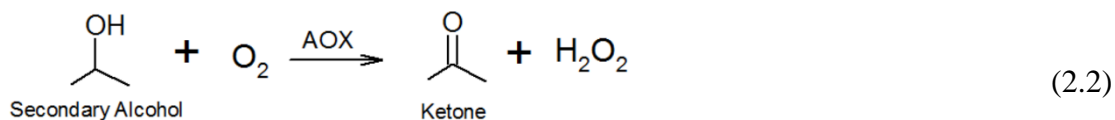
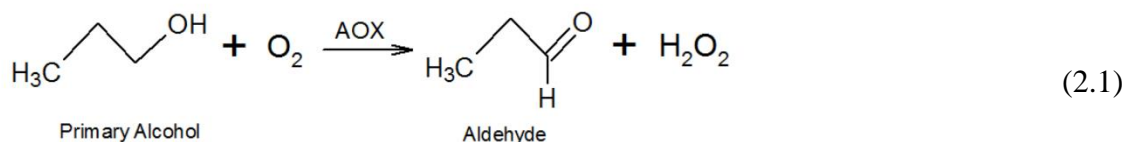
INCREASED STABILITY OF ALCOHOL OXIDASE UNDER HIGH HYDROSTATIC PRESSURE

Introduction

The ability to rapidly identify and quantify ethanol with high sensitivity and selectivity is very important for the alcoholic beverage and food industries. As a result of fermentation, stored fruit pulps need to measure ethanol for regulatory purposes (Nunes et al., 2016). Accurate quantification of alcohol, primarily ethanol, is also critical for medical and forensic applications, such as the analysis of human breath and blood (Patel et al., 2001). Practical quantification methods are also needed for onsite environmental analysis of transportation accidents involving ethanol consumption (Personna et al., 2013). Conventional alcohol measurements for the food industry, lack the speed and/or cost efficiency needed for quality assurance, because they frequently require expensive equipment and trained technicians to perform complex sample preparation. These techniques include gas chromatography, liquid chromatography, gravimetric techniques, dichromate oxidation, or measurements based on light refraction, and spectroscopy (AOAC, 2012).

Alcohol oxidase (AOX) is a homooctameric flavoprotein with a molecular weight of 600 – 675 kDa produced by methylotrophic microorganisms (Couderc and Baratti, 1980). Alcohol oxidase catalyzes the irreversible oxidation of alcohols to their corresponding aldehyde (Equation 2.1) or ketone (Equation 2.2) in the presence of oxygen. Biosensors based on AOX have the potential to overcome the hurdles associated with current food quality assurance

techniques, because of the specificity for alcohols and inherent speed of catalytic activity (Azevedo et al., 2005). Current AOX alcohol biosensors can produce quantitative results within one minute with sensitivities as low as $150 \mu\text{A mM}^{-1} \text{cm}^{-2}$ (Chinnadayala et al., 2014; Wen et al., 2007). However, due to the poor stability of AOX, alcohol biosensors experience rapid signal drift and loss of sensitivity, limiting their practical application in food processing.



Originally used as a non-thermal processing technique to inactivate damaging enzymes and harmful microorganisms, the use of high hydrostatic pressure (HHP) processing has expanded in the food industry. At varying pressure-temperature treatments, many enzymes have been stabilized by HHP (Eisenmenger and Reyes-De-Corcuera, 2009b). Undoubtedly, optimal conditions for stabilization of enzymes cover a large range of temperatures, pressures, substrates, pH, and solvents. Presently, no mathematical model based on the molecular structure of enzymes can predict how each enzyme behaves at HHP. Therefore, empirical models must be built based on experimentation.

In order to increase the longevity of AOX biosensors, strategies to stabilize AOX need to be developed. To the best of our knowledge, the effect of HHP on the stability of alcohol oxidase has not been previously studied. The hypothesis for this study was that HHP increases the

thermal stability of AOX. The objective of this research was to determine an optimum HHP that best stabilizes alcohol oxidase at selected temperatures.

Materials and Methods

Materials and Equipment

Alcohol oxidase from *Pichia pastoris* (Product Number A2404-1KU) and peroxidase from horseradish (POD, Product Number P8250-25KU), were purchased from the Sigma-Aldrich Chemical Company (St. Louis, MO, USA). Methanol (99.9%, Product Number A412-4) and potassium phosphate monobasic (Product Number P825-500) were purchased from Fisher Scientific (Fair Lawn, NJ, USA). 2,2'-Azino-bis(3-ethylbenzothiazoline-6-sulfonic acid) diammonium salt (ABTS, 98%) was purchased from Alfa Aesar (Ward Hill, MA, USA). Low-density polyethylene storage bags were cut and heat-sealed into 2 x 2 cm flexible containers for AOX solution during treatment in the reactor of the HHP system.

The HHP system, Figure 2.1, consisted of a high pressure micropump (model MP5), an 8.5-mL high pressure reactor (model U111), and a pump controller (MP5 micropump control unit) all from Unipress Equipment (Warsaw, Poland). Water baths, Isotemp 6200 R28 (10 °C) and Isotemp 6200 H11 (49.4 – 62.4 °C) from Fisher Scientific (Pittsburgh, PA, USA) were used to feed water into the jacket of the HHP reactor to control temperature. Sirai 3/2 – NC-NO S307 solenoid pinch valves (Bussero, Italy) controlled which water bath fed the reactor jacket depending on desired temperature. Temperature was monitored by a type K thermocouple, which protruded into the HHP reactor through the bottom, with the tip at the edge of the internal cavity of the reactor. Process times, pressures and solenoid valves were automatically controlled using a computer program written in LabVIEW 2014 with a data acquisition board (NI cDAQ 9174) from National Instruments (Austin, TX, USA). The LabVIEW program recorded the process

time, pressure, and temperature of the HHP reactor during treatment. BioTek's Synergy™ HTX Multi-Mode Microplate Reader (VT, USA) monitored the enzymatic assay absorbance change with a xenon flash lamp and monochromator at 405 nm. Data collection was performed with BioTek's Gen5 Data Analysis Software.

High Hydrostatic Pressure Processing

A 100- μ L sample of AOX solution (0.5 or 1.5 unit mL⁻¹ in 0.1 M potassium phosphate buffer at pH 7.5) was placed into the prepared plastic pouches, heat-sealed, and submerged in the HHP reactor at 10 °C. Sil 180 silicone oil bath liquid (Thermo Scientific, Rockford, IL, USA) was added to fill the reactor and then the reactor was closed with its threaded cap. Pressurization of the reactor was then initiated. Once the set point pressure was reached, the temperature was increased by switching to the second water bath previously set to the desired temperature. Process time began once the temperature reached 95% of the temperature set point. Figure 2.2 illustrates the pressure and temperature profile for a sample treated at 59.1 °C at 200 MPa for 0 (closed symbols) and 10 min (open symbols). To determine 100% residual activity for a process time of 0 min the reactor was cooled to 15 °C immediately after 95% of the set point temperature was reached. This initiated depressurization of the reactor as cooling continued to 10 °C. The sample was quickly removed and analyzed for activity.

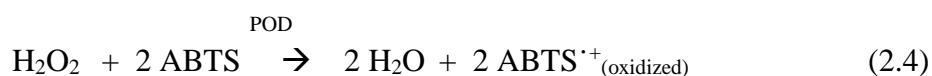
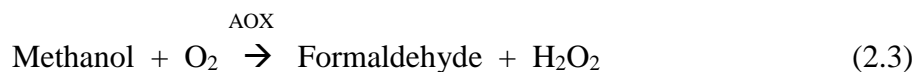
Processing Conditions

Samples were treated from 0.1 (control) to 200 MPa at 40 MPa increments at 49.4 °C, 52.6 °C, 55.8 °C or 59.1 °C. The Arrhenius equation was used to calculate the activation energy at each pressure; hence, temperature increments were chosen for uniform distribution of the reciprocal of the absolute temperature. Samples were treated at four process times adjusted for each temperature to produce an approximate 80% reduction of the residual activity after the

longest process time for each pressure-temperature combination. A randomized block design with temperatures treated as blocks was used. Pressure-time combinations for each temperature block were randomly selected and each treatment was done in duplicate.

Activity Measurements

A bi-enzymatic assay measured the activity of AOX spectrophotometrically at 25 °C. The production of H₂O₂ by the AOX catalyzed reaction (Equation 2.3) was monitored at 405 nm by the POD catalyzed oxidation of ABTS to the radical cation ABTS^{•+} (Equation 2.4, $\epsilon_{405} = 36,800 \text{ M}^{-1} \text{ cm}^{-1}$). One unit of AOX activity was defined as the amount of enzyme that causes the oxidation of 1 μmol of methanol to formaldehyde per min at pH 7.5 and 25 °C (Janssen and Ruelius, 1968; Keeseey, 1987). Methanol was selected as the substrate because of AOX's high specificity for the short-chained molecule and for the purpose of comparison with the literature since it is the substrate most commonly used in the enzymatic activity assay (Couderc and Baratti, 1980). The change in absorbance was recorded immediately after a 10- μL aliquot of the treated AOX sample was added and mixed to the reaction mixture containing 160 μL of 3.125 mM ABTS, 40 μL of 312.5 mM methanol and 40 μL of 4.5 unit mL^{-1} of POD (one unit of POD will form 1.0 mg of purpurogallin from pyrogallol in 20 s at pH 6.0 at 20 °C). The ABTS and methanol were auto-injected by the microplate reader, while the POD and AOX were manually pipetted into four wells per sample. Total reaction mixture volume was 250 μL per well. Methanol and POD were prepared with ultrapure water and ABTS and AOX solutions were prepared in 0.1 M potassium phosphate buffer at pH 7.5.



When not in use, all reagents were stored at 4 °C and enzymes were held on ice during the experiments. For all absorbance readings, the sample's pathlength was calculated by the ratio of the sample's change in absorbance between 977 nm and 900 nm over water's change in absorbance between 977 nm and 900 nm. The POD was needed in the reaction mixture to rapidly remove the hydrogen peroxide, since the presence of H₂O₂ inhibits the activity of AOX (Azevedo et al., 2004b).

Rate of Enzyme Inactivation

First and second reaction orders were analyzed to fit the rate of inactivation of AOX. The Arrhenius equation (Equation 2.5) was used to calculate the activation energy for AOX at each pressure:

$$\ln(k) = \left(-\frac{E_a}{R} \times \frac{1}{T} \right) + \ln(k_{T_o}) \quad (2.5)$$

where k is the rate constant, T is the absolute temperature, R is the ideal gas constant (8.3145 J mol⁻¹ K⁻¹), E_{ai} is the activation energy, k_{T_o} is the rate constant at a reference absolute temperature. The i was added to the symbol E_{ai} to denote this is an activation energy of inactivation, rather than activation energy of activation.

Eyring's equation (Equation 2.6) was used to calculate the activation volume of AOX at each temperature tested with the rates of inactivation:

$$\ln(k_o) = \left(\frac{\Delta V^\ddagger}{RT} \times P \right) + \ln(k_{P_o}) \quad (2.6)$$

where k_o is the rate constant, P is the pressure, ΔV^\ddagger is the activation volume, and k_{P_o} is the rate constant at reference pressure P_o .

Error for rates of inactivation, activation energies and activation volumes was reported as the standard error of the linear regression.

Results and Discussion

Enzyme Inactivation

The first AOX inactivation study is illustrated in Figure 2.3 where the first-order rates of thermal inactivation of AOX at 45 °C and 50 °C and atmospheric pressure are plotted as the logarithm of the residual activity *versus* time. Table 2.1 displays the calculated first- and second-order rates of inactivation for AOX, as well as their correlation coefficients. The correlation coefficients at 45 °C were equal for both first- and second-order models at 0.72. At 50 °C the correlation coefficient for the first-order model at 0.74 was greater than that of the second-order model at 0.59. Consequently, all rates of inactivation are calculated as pseudo-first-order models henceforth.

Importantly, Figure 2.3 revealed two linear regions of inactivation for AOX at both temperatures, suggesting two populations of enzyme. Table 2.1 also presents the rates of inactivation for both linear regions, k_1 (0 to 2 min process time) and k_2 (4 to 10 min process time). Reduced rate of inactivation is demonstrated by the 4-fold reduction between k_1 and k_2 at 45 °C and the 3.5-fold reduction at 50 °C. The correlation coefficients for the two-region interpretation of the data were quite low, less than 0.4, except for k_1 at 50 °C with 0.78. These low results were attributed to few data points as a result of the preliminary nature of this work.

For the remainder of this study, the two regions were investigated individually in order to accurately describe their rates of inactivation. The first region of thermal inactivation of AOX is

more thermolabile and referred to as the L fraction, the second more thermoresistant region is referred to as the R fraction. The L fraction was analyzed at process times between 0 and 3 min at an enzyme concentration of 0.5 unit mL⁻¹. The R fraction was analyzed at process times between 4 to 20 min at an enzyme concentration of 1.5 unit mL⁻¹. Process times for each fraction were based on the time frames of the two regions exposed during preliminary thermal inactivation of AOX at atmospheric pressure and HHP. Attributed to the longer process times, a higher enzyme concentration was used for the R fraction, to ensure AOX activity was spectrophotometrically detectable for each pressure-temperature treatment.

The two-regions observed during the AOX thermal inactivation have been previously described as a “series model,” where the stable homooctamer of AOX quickly converts during thermal inactivation to an active intermediate form, which eventually denatures completely (Azevedo et al., 2004b; Gianfreda et al., 1984). Another explanation is the enzyme in fact being a mixture of isoenzymes with different heat sensitivities known as “parallel model” (Aymard and Belarbi, 2000; Greco and Gianfreda, 1984). For this study a purified enzyme was used, suggesting a dissociation of the AOX into stable structures rather than isozymes.

Stabilization Effect of High Hydrostatic Pressure

Figure 2.4 shows the nonlinear decrease of AOX activity for the L region as a function of processing time at 52.6 °C for the selected pressures of 0.1, 40, 80 and 120 MPa. As pressure increased more activity was retained indicating the stabilization effect of HHP. Notably, a 3-fold increase in the residual activity of AOX after 2 min at 52.6 °C and 120 MPa at 58.5 % as compared to atmospheric pressure at 19.4 %.

High hydrostatic pressure stabilized the L fraction at 49.4 and 52.6 °C. For the R fraction HHP provided stabilization for temperatures between 49.4 and 59.1 °C. Pseudo-first order rate

constants of AOX inactivation are provided in Table 2.2. It was concluded that the slowest rates of inactivation were seen at a range of pressures between 80 to 200 MPa, but generally concentrated between 120 and 160 MPa. The transition from stabilization to destabilization by pressure occurred at pressures greater than 160 MPa for AOX.

Multiple mechanisms are thought to contribute to pressure-induced stabilization of enzymes against thermal inactivation. Predominantly, stabilization is thought to occur due to antagonistic effects of increasing pressure and increasing temperature on the inter- and intramolecular interactions of enzymes (Mozhaev et al., 1996). Eisenmenger and Reyes-De-Corcuera (2009a) explained this opposing effect in molecular terms where temperature increases entropy, while increase in pressure increases order, thus decreases entropy. Furthermore, HHP increases the hydration of an enzyme's charged and non-polar groups hampering water loss, which has been hypothesized as an initial step of thermal inactivation as a result of high temperature (Balny et al., 2002; Boonyaratanakornkit et al., 2002). Additionally, heat disrupts hydrogen bonds, while HHP has been thought to enhance and promote formation of hydrogen bonds (Eisenmenger and Reyes-De-Corcuera, 2009b).

Activation Energy of Inactivation

The Arrhenius equation was used to calculate the apparent activation energy of inactivation (E_{ai}). Figure 2.5 and Figure 2.6 illustrate the linear relationship of the logarithm of the rate constant and the reciprocal of absolute temperature for the L and R fraction, respectively. Table 2.3 reports the E_{ai} for 40 to 200 MPa at 40 MPa increments for both L and R focused regions of AOX inactivation. For the L fraction apparent E_{ai} increased as pressure increased from 40 to 160 MPa, followed by a decrease at 200 MPa. For the R fraction the apparent E_{ai} increases as pressure continued to increase from 40 to 120 MPa, then persisted to decrease at 160 and 200

MPa. The R fraction had a reduced sensitivity to temperature change than the L fraction at all pressures as indicated by a 21 to 51% difference in the E_{ai} for the corresponding pressure. The E_{ai} 's at 200 MPa for the L and the R fraction were not different when considering the standard error calculated from the linear regression. At pressures between 0.1 and 160 MPa the calculated E_{ai} 's for L and R did differ. Notably, the E_{ai} for 40 to 200 MPa were not different when considering the standard error calculated from the linear regression used to determine E_{ai} , for the R fraction. For the L fraction, only the E_{ai} for 200 MPa was different from the other selected pressures when considering the standard error calculated from the linear regression indicating at 200 MPa high pressure is acting more as an additive denaturant rather than a stabilizing force.

Lopez-Gallego et al. (2007) reported figures of residual activity *versus* time for AOX from *Pichia pastoris* at 37 °C and 45 °C at atmospheric pressure, pH 7 and enzyme concentration of 0.1 mg mL⁻¹. An estimate of the rates of inactivation at 37 °C and 45 °C allowed for the E_{ai} to be calculated. The E_{ai} was approximately 111 kJ mol⁻¹. For the L fraction at 0.1 MPa and 55.8 °C and 59.1 °C the rates of inactivation were so fast that they were not able to be determined experimentally. The initial activity for the R fraction was determined after a 4 min process time, producing activities too low to determine rates of inactivation experimentally at 0.1 MPa for all selected temperatures. The lack of rates of inactivation at 0.1 MPa resulted in the inability to calculate E_{ai} at 0.1 MPa for either protein fraction. Thus a comparison of E_{ai} between this study and Lopez-Gallego et al. (2007) was unavailable. The decreasing trend for E_{ai} with decreasing pressure for the L region does indicate that two E_{ai} 's would be similar.

Activation Volume

Figure 2.7 and Figure 2.8 depict the linearized effect of pressure on the rate of inactivation for the L and R fraction, respectively. As pressure increased the rate of inactivation

decreased up to around 160 MPa. The downward trending slope between 40 and 120 MPa was used to calculate the apparent ΔV^\ddagger for each temperature and protein fraction. The ΔV^\ddagger 's for 49.4 and 52.6 °C of the L fraction were an exception and the ΔV^\ddagger was calculated between 0.1 and 120 MPa because at 0.1 MPa rates of inactivation were experimentally determined. The data for 160 MPa was excluded to avoid inaccurately decreasing the ΔV^\ddagger due to the transition phase nature between 120 and 200 MPa. The transition phase is the range of high pressures that stop increasing stabilization of AOX, but begins to destabilize the enzyme. Utilizing the calculated ΔV^\ddagger , reported in Table 2.4, the rates of inactivation at 0.1 MPa that were not determined experimentally for the L and R fractions were determined by extrapolation.

Activation volume was greatest at 49.4 °C for the L fractions at 46.6 cm³ mol⁻¹ and at 55.8 °C at 23.9 cm³ mol⁻¹ for the R fraction. The ΔV^\ddagger for the R fraction at 49.4 °C was similar to that of 55.8 °C at 22.2 cm³ mol⁻¹. At 52.6 °C the ΔV^\ddagger decreased to 22.3 cm³ mol⁻¹ for the L fraction and 8.6 cm³ mol⁻¹ for the R fraction. For the L fraction at 55.8 and 59.1 °C and for the R fraction at 59.1 °C, the negative or low ΔV^\ddagger with high standard error signify a negligible stabilization effect of HHP for AOX.

Boonyaratanakornkit et al. (2002) described how specific molecular interactions at HHP for each enzyme determine the magnitude and sign of ΔV^\ddagger . However, these interactions, such as electrostriction of charged and polar groups and the solvation of hydrophobic groups, are often difficult to pinpoint. Positive ΔV^\ddagger 's, 13.7 and 33.7 cm³ mol⁻¹, were observed during thermostabilization of a pectinase cocktail from *Aspergillus niger* with pressures up to 250 MPa and temperature range of 55 to 85 °C (Tomlin et al., 2013). The ΔV^\ddagger had a general increase until 77 °C where the highest ΔV^\ddagger occurred. A decrease in ΔV^\ddagger at 85 °C indicated pressure having less of an effect on thermostability. To more accurately determine trends for the ΔV^\ddagger of AOX for

both the L and R fraction, data is needed at 80 and 100 MPa and lower temperatures should be tested.

Thermolabile Fraction versus Thermoresistant Fraction of Alcohol Oxidase

The residual activity for the R fraction, was normalized to 100% after a process time of 4 min under selected pressure-temperature conditions that resulted in complete inactivation of the L fraction. This facilitates the comparison between the two fractions as shown in Figure 2.9 which illustrates the greatest difference in rate of inactivation between the L and R fractions. At 55.8 °C and 80 MPa, the rate of inactivation for the R fraction, 0.040 min⁻¹, was 34 times slower than the rate of inactivation for the L fraction at 1.356 min⁻¹, highlighting the difference between the thermolabile and thermoresistant regions of thermal inactivation.

At 49.4 °C and 52.6 °C for the L fraction, HHP (40 to 200 MPa) stabilized the enzymes as compared to the control. At 49.4 °C at 160 MPa and 52.6 °C at 120 MPa, the L fraction exhibited a 14.6-fold and 2.6-fold increase in stability, respectively, as compared to atmospheric pressure. Due to small apparent ΔV^\ddagger for the L fraction at 55.8 °C and 59.1 °C, their calculated rates of inactivation at 0.1 MPa were more stable than the rates of inactivation at 80 MPa for 55.8 °C and 40 MPa at 59.1 °C. All high pressure treatments stabilized AOX for the R fraction as compared to the calculated control at atmospheric pressure. The apparent rate of inactivation at atmospheric pressure for 49.4 °C and 52.6 °C for the R fraction, decreased 3-fold at 120 MPa and 1.4-fold at 160 MPa, respectively.

It should be noted that the 3-fold increase in AOX concentration, from 0.5 unit mL⁻¹ (0.02 mg mL⁻¹) for the L fraction to 1.5 unit mL⁻¹ (0.06 mg mL⁻¹) for the R fraction, was assumed to not have a great impact on the stability against thermal inactivation. This was supported by Azevedo et al. (2004b) who reported that a 10-fold increase in AOX from concentration (0.025

to 0.25 mg mL⁻¹) did not impact the rate of thermal inactivation. In contrast, Lopez-Gallego et al. (2007) established that a 10-fold increase in AOX concentration (0.01 to 0.1 mg mL⁻¹) increased the stability to thermal inactivation, proposing a dissociation of the subunits as an initial step of inactivation.

Another multimeric oxidoreductase, polyphenoloxidase (PPO) has been effectively stabilized with HHP. Dalmadi et al. (2006) described PPO from strawberries (*Fragaria ananassa*), a tetrameric enzyme, to have a thermolabile and thermoresistant fraction. At temperatures (>50 °C) and low pressures (≤200 MPa) enzyme stabilization was observed. At 60 °C the rate of inactivation for the stable fraction decreased 13.8-fold from 0.1 MPa as compared to 200 MPa. Similarly, polyphenoloxidase from avocado was stabilized at temperatures greater than 62.5 °C and pressures lower than 250 MPa (Weemaes et al., 1998). A 16.6-fold stabilization occurred at 72.5 °C at 250 MPa as compared to 0.1 MPa. The PPO from avocado was not described to have two fractions with different stabilities.

Conclusions

During AOX thermal inactivation (49.4 °C to 59.1 °C) at atmospheric and HHP two pseudo-first order rates of inactivation were observed. The two regions were associated with intrinsic thermolabile and thermoresistant fractions of AOX. High pressure treatments of 80 to 200 MPa stabilized AOX, with the slowest rates of inactivation generally concentrated between 120 MPa and 160 MPa. Destabilization by pressure occurred at pressures greater than 160 MPa for AOX. The optimal thermo-stabilization of AOX between 120 and 160 MPa can be used in combination with immobilizing techniques to develop electrochemical biosensors with increased longevity.

Table 2.1. Comparison of the kinetic rates of alcohol oxidase thermal inactivation at 45 °C and 50 °C for first- and second-order models for one-region and first-order model for two-regions at atmospheric pressure at an enzyme concentration of 0.1 unit mL⁻¹.

45 °C				50 °C			
1st Order				1st Order			
k ₁ (min ⁻¹)	0.11	R ²	0.72	k ₁ (min ⁻¹)	0.28	R ²	0.74
2nd Order				2nd Order			
k ₁ (min ⁻¹)	0.002	R ²	0.72	k ₁ (min ⁻¹)	0.02	R ²	0.59
Two-Region (1st order)				Two Region (1st order)			
k ₁ (min ⁻¹)	0.20	R ²	0.39	k ₁ (min ⁻¹)	0.66	R ²	0.76
k ₂ (min ⁻¹)	0.05	R ²	0.27	k ₂ (min ⁻¹)	0.19	R ²	0.38

Table 2.2. Pseudo-first order rate of alcohol oxidase inactivation \pm standard error determined by the linear regression of residual activity *versus* process time.

Pressure (MPa)	Temperature (°C)							
	49.4 L	49.4 R	52.6 L	52.6 R	55.8 L	55.8 R	59.1 L	59.1 R
k (min ⁻¹)								
0.1	0.655 ^a \pm 0.139	0.030*	0.567 ^a \pm 0.105	0.040*	0.844*	0.093*	1.128*	0.059*
40	0.147 ^b \pm 0.006	0.019 ^a \pm 0.004	0.425 ^b \pm 0.067	0.037 ^{a,b} \pm 0.012	0.788 ^a \pm 0.074	0.070 ^a \pm 0.012	1.034 ^a \pm 0.176	0.053 ^a \pm 0.009
80	0.080 ^c \pm 0.021	0.020 ^a \pm 0.002	0.287 ^c \pm 0.032	0.029 ^{a,b} \pm 0.009	1.356 ^b \pm 0.120	0.040 ^b \pm 0.006	0.719 ^{b,c} \pm 0.076	0.066 ^a \pm 0.014
120	0.079 ^c \pm 0.024	0.010 ^b \pm 0.002	0.216 ^d \pm 0.041	0.028 ^b \pm 0.005	0.933 ^a \pm 0.150	0.035 ^{b,c} \pm 0.003	0.756 ^b \pm 0.072	0.051 ^a \pm 0.011
160	0.045 ^d \pm 0.025	0.012 ^b \pm 0.004	0.245 ^{d,e} \pm 0.023	0.027 ^b \pm 0.008	0.831 ^a \pm 0.145	0.031 ^c \pm 0.005	0.749 ^{b,c} \pm 0.119	0.055 ^a \pm 0.010
200	0.201 ^e \pm 0.029	0.018 ^a \pm 0.004	0.270 ^{c,e} \pm 0.031	0.034 ^a \pm 0.004	0.815 ^a \pm 0.102	0.031 ^c \pm 0.006	0.651 ^{b,c} \pm 0.103	0.065 ^a \pm 0.012

^{a-c} Represent a difference in rate of AOX inactivation determined by \pm standard error calculated from the linear regression for each temperature and protein fraction, L and R.

* Represents rate constants which were calculated from the temperature and protein fraction's activation volume.

Table 2.3. Effect of temperature on rate of alcohol oxidase thermal inactivation.

Pressure (MPa)	L		R	
	E_{ai} (kJ mol ⁻¹)	R ²	E_{ai} (kJ mol ⁻¹)	R ²
40	178.7 ^a ± 34.3	0.93	105.1 ^a ± 45.5	0.73
80	224.1 ^a ± 96.1	0.73	107.5 ^a ± 7.1	0.99
120	227.0 ^a ± 67.4	0.85	144.4 ^a ± 36.9	0.88
160	266.4 ^a ± 80.0	0.85	127.9 ^a ± 21.5	0.95
200	127.6 ^b ± 47.6	0.78	101.3 ^a ± 31.3	0.84

^{a-b} Different letters represent a difference in activation energy determined by ± standard error calculated from the linear regression for each pressure and protein fraction, L and R.

Table 2.4. Effect of pressure on rate of alcohol oxidase thermal inactivation.

Temperature (°C)	L		R	
	ΔV^\ddagger (cm ³ mol ⁻¹)	R ²	ΔV^\ddagger (cm ³ mol ⁻¹)	R ²
49.4	46.6 ^a ± 15.8	0.81	22.2 ^a ± 15.9	0.66
52.6	22.3 ^a ± 1.0	1.00	8.6 ^{ab} ± 4.3	0.80
55.8	-5.8 ^b ± 18.1	0.09	23.9 ^a ± 8.4	0.89
59.1	10.8 ^b ± 8.2	0.63	1.4 ^b ± 9.5	0.02

^{a-c} Represent a difference in activation volume determined by ± standard error calculated from the linear regression for each temperature and protein fraction, L and R.

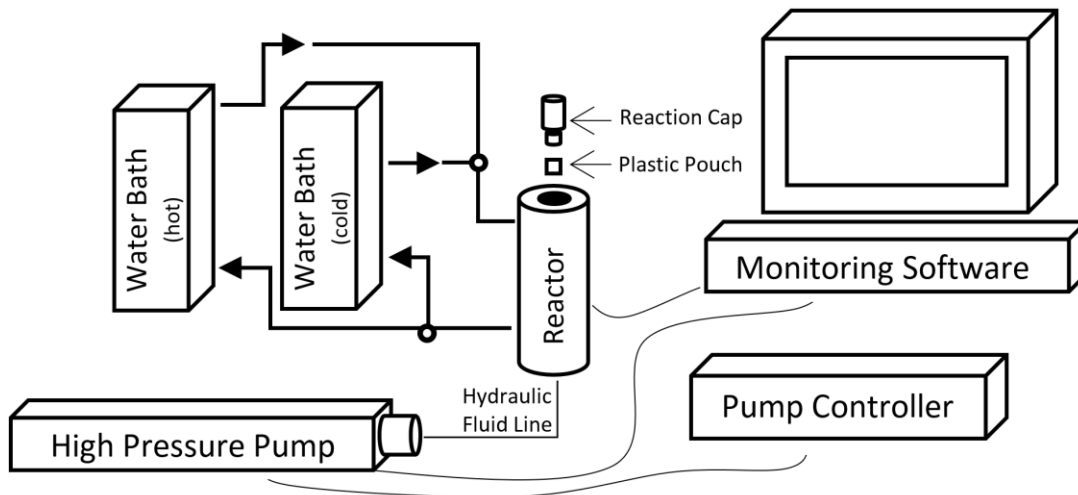


Figure 2.1. High hydrostatic pressure equipment schematic.

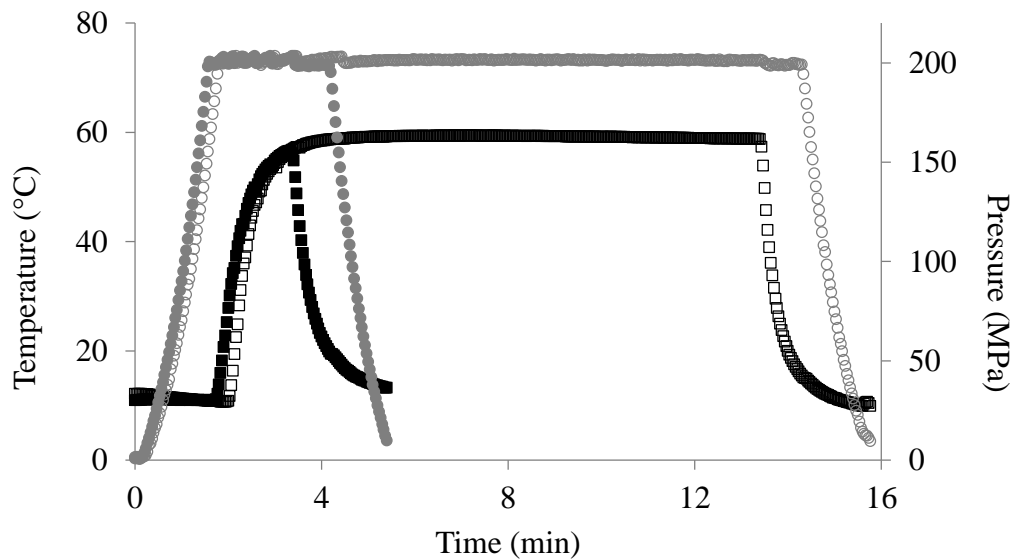


Figure 2.2. Pressure (○) and temperature (□) profiles in high pressure reactor for sample treated at 59.1 °C at 200 MPa for 10 min and pressure (●) and temperature (■) profiles for treatment at 59.1 °C at 200 MPa for 0 min.

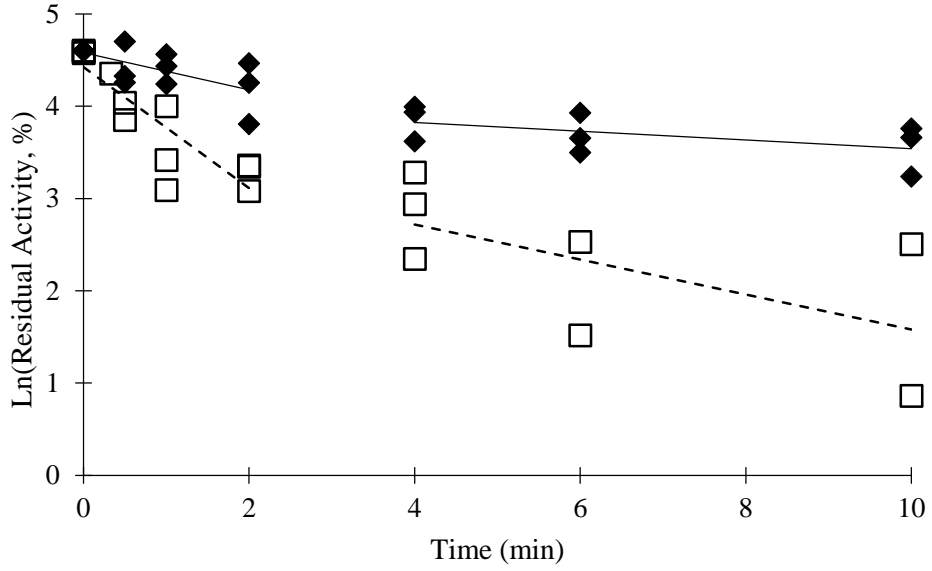


Figure 2.3. Alcohol oxidase rate of inactivation at atmospheric pressure and 45.0 °C (◆) and 50.0 °C (□) at an enzyme concentration of 0.1 unit mL⁻¹.

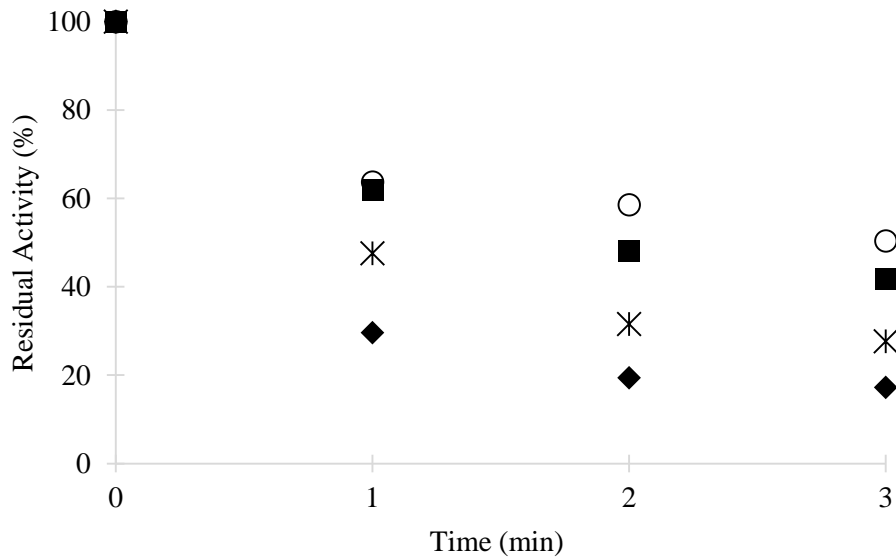


Figure 2.4. Effect of high hydrostatic pressure on residual activity of L region at 52.6 °C for treatment at 0.1 MPa (◆), 40 MPa (✕), 80 MPa (■), 120 MPa (○).

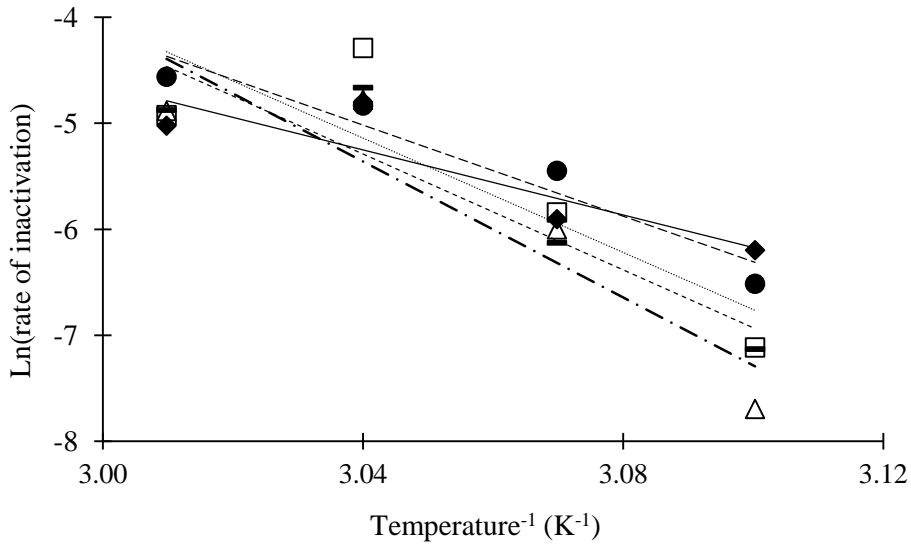


Figure 2.5. Arrhenius plot for AOX thermal inactivation of the L fraction at 40 MPa (●), 80 MPa (◻), 120 MPa (---), 160 MPa (△), 200 MPa (◆), Values on x-axis x 10³

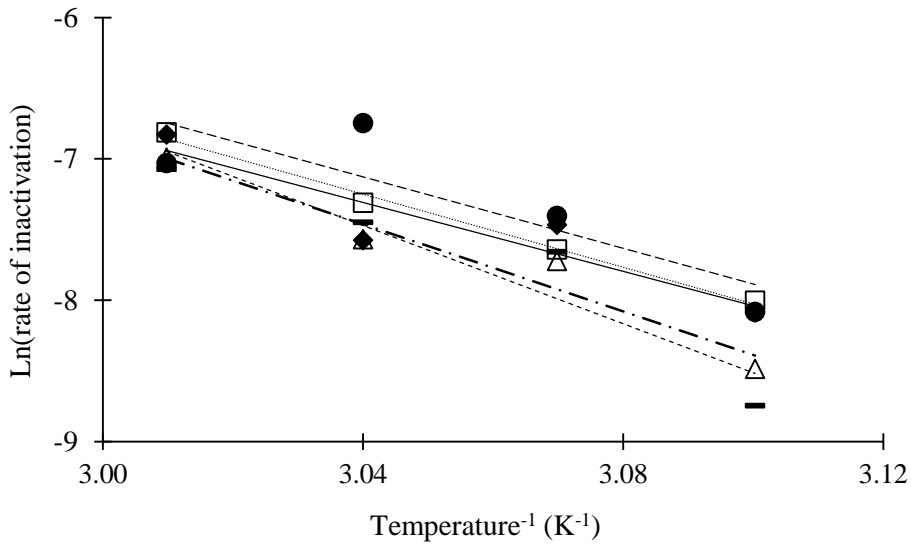


Figure 2.6. Arrhenius plot for AOX thermal inactivation of the R fraction at 40 MPa (●), 80 MPa (◻), 120 MPa (---), 160 MPa (△), 200 MPa (◆), Values on x-axis x 10³.

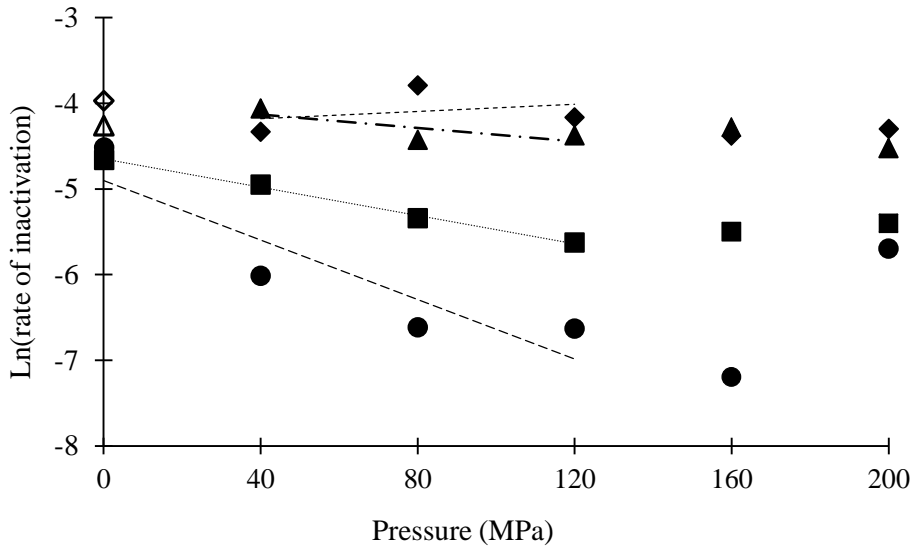


Figure 2.7. Eyring plot for AOX thermal inactivation of the L fraction at 49.4 °C (●), 52.6 °C (■), 55.8 °C (◆), 59.1 °C (▲), open symbols signify a calculated rate constant at 0.1 MPa.

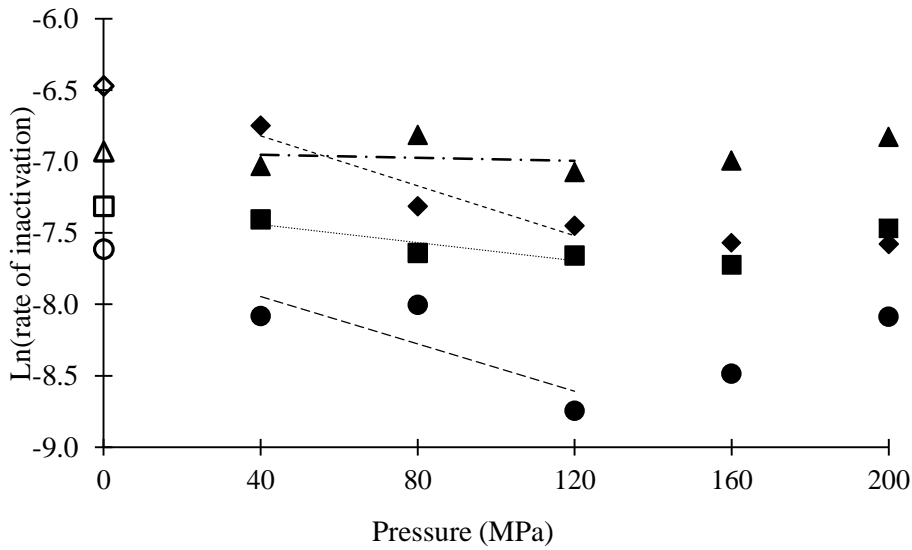


Figure 2.8. Eyring plot for AOX thermal inactivation of the R fraction at 49.4 °C (●), 52.6 °C (■), 55.8 °C (◆), 59.1 °C (▲), open symbols signify a calculated rate constant at 0.1 MPa.

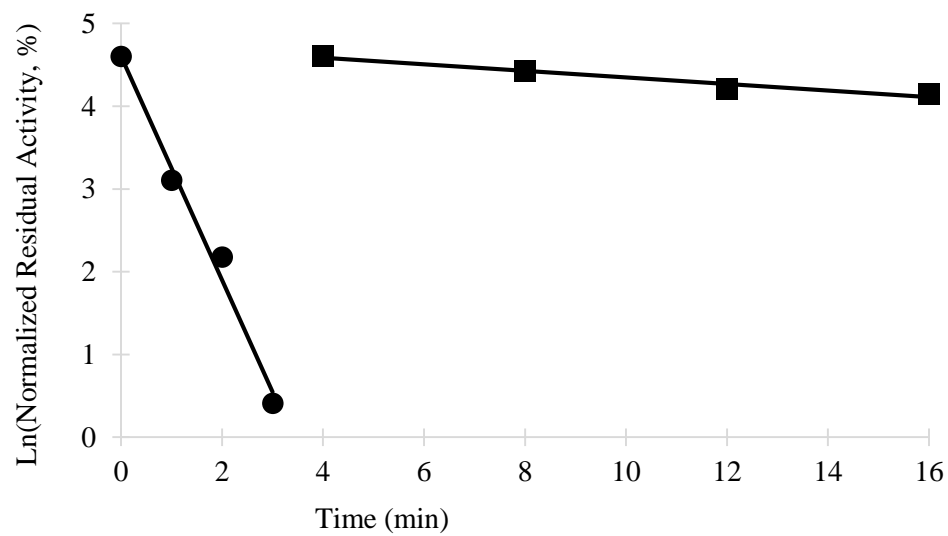


Figure 2.9. A comparison of the rates of AOX inactivation at 80 MPa and 55.8 °C for L fraction at 0.5 unit mL⁻¹ (●) and R fraction 1.5 unit mL⁻¹ (■).

CHAPTER 3

INCREASED ACTIVITY OF ALCOHOL OXIDASE AT HIGH HYDROSTATIC PRESSURE

Introduction

Expensive aldehydes that can serve as precursors of other fine chemicals or flavor compounds can be naturally produced by alcohol oxidase (AOX). For example, whole cells of *Pichia pastoris* containing AOX oxidized endogenous alcohols in orange water phase essence to produce acetaldehyde, propanal and octanal improving the sensory attributes, ergo the value (Goodrich et al., 1998). The important almond associated flavor, benzaldehyde, can also be produced by AOX through the oxidation of benzyl alcohol (Duff and Murray, 1989; Fujii and Tonomura, 1972). Glycolaldehyde is used to synthesize serines, tryptophan, agrochemicals and medicine (Ukeda et al., 1998). While chemical methods of production have limitations including low conversion yields and high reaction temperature, glycolaldehyde can be produced from ethylene glycol by AOX with high conversion yields and selectivity (Isobe and Nishise, 1995). Other chemicals that can be produced by AOX include glyoxal, hexanal, octanal, 3-phenylpropanal, and phenyl acetaldehyde (Isobe and Nishise, 1995; Murray and Duff, 1990).

Numerous enzymes have shown an increase in stability and enzymatic rate at HHP (Eisenmenger and Reyes-De-Corcuera, 2009b). An increase in AOX activity could result in the rapid and natural production of these valuable chemicals. High hydrostatic pressure (HHP) can in some cases also increase the catalytic activity of enzymes. Organized into three groups

Eisenmenger and Reyes-De-Corcuera (2009b) summarized how pressure can change enzyme reaction rate: 1) direct change of enzyme structure, 2) reaction mechanism changes, 3) solvent or substrate physical property changes that could affect group 1 or 2. However, presently, to the best of our knowledge no published work describes the effect of HHP on the rate of AOX-catalyzed reactions. The hypothesis for this study was that HHP increases the catalytic activity of AOX. The objective of this study was to assess the effect of HHP on the activity of AOX at selected temperatures for the production of formaldehyde from methanol.

Materials and Methods

Materials and Equipment

All reagents used for this experiment were the same as those in Chapter 2 and prepared at the same concentrations unless noted. Methanol was selected as the substrate because of AOX's high specificity for the short-chained molecule and for the purpose of comparison with the literature since it is the substrate most commonly used in the enzymatic activity assay (Couderc and Baratti, 1980). The HHP equipment setup, Figure 3.1, was similar to that of Chapter 2. Instead of the high pressure reactor (model U111), a 1.9-mL high pressure optical vessel (model U103) with sapphire windows from Unipress Equipment (Warsaw, Poland) was used. Water baths, Isotemp 6200 R28 (10 °C) and Isotemp 6200 H11 (37.0 – 59.1 °C) from Fisher Scientific (Pittsburgh, PA, USA) were used to feed water into the jacket of the high pressure optical vessel to control temperature. Sirai 3/2 – NC-NO S307 solenoid pinch valves (Bussero, Italy) controlled which water bath fed the reactor jacket depending on desired temperature. An Ocean Optics, Inc. (Dunedin, FL, USA) HR4000CG-UV-NR high resolution spectrophotometer with a DH-2000-UV-vis-NIR light source with deuterium and halogen lamps was connected via fiber optic cables

to the high pressure optical cell. Ocean Optics OceanView 1.5.0v software was used to collect absorbance readings at 405 nm.

The reaction mixture was prepared and placed in a cylindrical quartz cuvette with ID of 7.4 mm, OD of 9.6 mm and length of 20.8 mm. Teflon™ stoppers were used to plug the top and bottom of the cuvette. Both Teflon™ stoppers were made out of a 0.7 cm diameter rod cut to 1 cm in length. A groove in the middle of the stopper was etched and an O-ring was tightly situated into the etched space. The O-rings ensured a water tight seal at the top and bottom of the quartz cuvette. The cuvette held a volume of 350 μL with the stoppers in place. Temperature was measured using a type K thermocouple which protruded through the side of the reactor with the tip at the edge of the internal cavity of the reactor.

In-Situ Activity Measurement at High Hydrostatic Pressure

The reaction mixture contained 14 μL of AOX solution (0.063 unit mL^{-1} or 0.074 unit mL^{-1} in 0.1 M potassium phosphate buffer at pH 7.5), 218 μL of 3.125 mM ABTS, 54 μL of 312.5 mM methanol and 54 μL of 4.5 unit mL^{-1} of POD. One unit of AOX activity was defined as the amount of enzyme that causes the oxidation of 1 μmol of methanol to formaldehyde per min at pH 7.5 and 25 $^{\circ}\text{C}$ (Janssen and Ruelius, 1968; Keeseey, 1987). One unit of POD will form 1.0 mg of purpurogallin from pyrogallol in 20 s at pH 6.0 at 20 $^{\circ}\text{C}$. Total reaction mixture volume was 340 μL . Methanol and POD were prepared with ultrapure water and ABTS and AOX solutions were prepared in 0.1 M potassium phosphate buffer at pH 7.5. Care was taken to avoid the entrapment of air bubbles when closing the top stopper of the vial. The vial was submerged in the silicone oil filled HHP reactor at 5 $^{\circ}\text{C}$. The reactor was then sealed with the threaded cap. Pressurization of the reactor was initiated 45 s after AOX had been added to the reaction mixture for every sample to ensure consistency. Change in absorbance was measured *in-*

situ once pressure set point and 95% of temperature set point had been reached for a time frame up to 5 min.

V_{max} Calculation

According to the Michaelis-Menten equation if the substrate concentration is in excess of the K_m the reaction will perform at max velocity. Equation 3.1 states the Michaelis-Menten equation:

$$v = \frac{V_{max} [S]}{K_m + [S]} \quad (3.1)$$

where v is the reaction velocity, V_{max} the maximum velocity of the reaction, $[S]$ the substrate concentration and K_m the Michaelis-Menten constant. The reagent concentrations as described in the *In-Situ Activity Measurement at High Hydrostatic Pressure* permits for the substrate to be in excess, because the $[S]$ is 50 mM, which is 25 times greater than the K_m at approximately 2 mM (Couderc and Baratti, 1980). Thus the AOX activity is equivalent to the V_{max} of the reaction. The rate constant or the initial change in absorbance *versus* time was used to calculate the V_{max} at selected pressure-temperature treatments using Beer's law (Equation 3.2).

$$A = \epsilon l c \quad (3.2)$$

where A is absorbance, ϵ is the molar absorptivity, l the pathlength and c the concentration of the solution. By measuring the change in absorbance over time due to H_2O_2 production, the change in concentration of substrate over time, the V_{max} , can be calculated.

Processing Conditions

To determine the effect of HHP on V_{max} , AOX at a concentration of $0.063 \text{ unit mL}^{-1}$, was treated at 0.1 (control) or 160 MPa (a pressure within the high pressure range that imparted the

greatest level of stabilization to the enzyme on Chapter 2) at 37.0, 40.9, 44.9, 49.0, or 53.2 °C. The Arrhenius equation was used to calculate the activation energy at each pressure; hence, temperature increments were chosen for uniform distribution of the reciprocal of the absolute temperature. The temperature 37.0 °C was used because it is the reported optimal temperature at atmospheric pressure for activity of AOX from *Pichia pastoris* (Couderc and Baratti, 1980).

The activation energy of activation (E_a) was also determined *in-situ* for AOX (0.074 unit mL⁻¹) at 0.1 MPa from 20.0 °C to 37.0 °C. A randomized block design with temperature treated as blocks was used. Pressure treatment was randomly selected and performed in triplicate for each temperature block. Statistical analysis of treatment methods was conducted using SAS statistical software (Cary, NC, USA) to perform analysis of variance and multiple comparison with Tukey's test ($\alpha=0.05$).

Results and Discussion

Alcohol Oxidase Activity

After 95% of the set point temperature was reached the V_{max} at selected treatment conditions was calculated from the linear portion of the change in absorbance over time. The change in absorbance at 0.1 MPa and 160 MPa between 37.0 °C to 53.2 °C over time was plotted in Figure 3.2 and Figure 3.3, respectively. Absorbance change was adjusted to 0 at time 0 for all temperature-pressure treatments for clarity and to compensate for the increase in absorbance during come up time. The change in absorbance increased over the five-minute reaction time, however, deviation from linearity occurred for both 0.1 and 160 MPa.

Prominently, at 0.1 MPa, the rate of reaction was no longer constant after 1 min for 49.0 and 53.2 °C. Table 3.1 provides the calculated V_{max} at all selected temperatures and both

pressures using the data from only the first minute of the recorded reaction. Deviations from linearity of absorbance *versus* time are less noticeable at 160 MPa because the pressure stabilized AOX against thermal inactivation. Illustrated by Figure 3.3, the rate of reaction at 53.2 °C is the fastest for the first 1.5 min, after which the rate deviates from linearity indicating thermal inactivation of AOX. Eisenmenger and Reyes-De-Corcuera (2009a), observed similar behavior for lipase at 71.8 °C and 80.0 °C while studying the activity difference at 0.1 MPa and 400 MPa. The deviation from linearity was suggested to be an indication of lipase thermal inactivation within the measured reaction time frame.

The deviation from linearity at both pressures is attributed to the high temperature of the reaction. Dependent on the pressure set point and temperature set point, activity is reduced during the come up time for the HHP equipment (explained in Chapter 2) because of the amount of time the reactor takes to reach the desired set point. Therefore, the estimates of V_{\max} are most likely underestimates but they are the best possible estimates based on the experimental setup.

Effect of High Hydrostatic Pressure on Alcohol Oxidase

The V_{\max} for every temperature tested was 65 to 141% greater at 160 MPa as compared to 0.1 MPa. A 3.2-fold increase in the V_{\max} was observed at 53.2 °C and 160 MPa as compared to the optimum temperature of 37.0 °C at atmospheric pressure (Couderc and Baratti, 1980). At 0.1 MPa there was significance differences in apparent V_{\max} between 37.0 °C to 53.2 °C. The V_{\max} of 4.4 $\mu\text{M min}^{-1}$ at 40.9 °C and 0.1 MPa was significantly greater than the V_{\max} at 37.0 and 44.9 °C at 2.6 and 2.8 $\mu\text{M min}^{-1}$, respectively. At 49.0 and 53.2 °C at 0.1 MPa slightly increased at 3.8 and 3.4 $\mu\text{M min}^{-1}$. At 160 MPa the V_{\max} at 53.2 °C, 8.2 $\mu\text{M min}^{-1}$ was significantly greater than the V_{\max} 's at 37.0 and 44.9 °C at 4.5 and 6.1 $\mu\text{M min}^{-1}$, respectively. The increase in V_{\max} at

53.2 °C represents a shift in optimum temperature for activity at 160 MPa as compared to 37 °C at 0.1 MPa, demonstrating the stabilizing effect of HHP.

A comparable increase in reaction rate at HHP was described by Tomlin et al. (2014). Specifically, the rate of viscosity reduction of pectin solutions with a commercial blend pectinase from *Aspergillus niger* increased 2.6 times under 300 MPa and 62.4 °C as compared to the traditional environment of use at 45 °C and atmospheric pressure. An impressive increase in catalytic activity was reported by Mozhaev et al. (1996) where α -chymotrypsin's activity with an anilide substrate at 50 °C and 360 MPa increased 30 times as compared to 20 °C at 0.1 MPa. In that study the activation volume increased from $-25 \text{ cm}^3 \text{ mol}^{-1}$ at 50 °C to $-10 \text{ cm}^3 \text{ mol}^{-1}$ at 20 °C. The large increase in activity of α -chymotrypsin was attributed to a strong temperature dependence of the reaction's activation volume (ΔV^\ddagger). Activation volume can be estimated using Eyring's equation (3.3)

$$\left(\frac{\partial \ln k}{\partial p}\right)_T = -\frac{\Delta V^\ddagger}{RT} \quad (3.3)$$

Where p is the pressure, T is the absolute temperature, R is the ideal gas constant ($8.3145 \text{ J mol}^{-1} \text{ K}^{-1}$), ΔV^\ddagger is the activation volume that represents the dependence of the reaction rate with pressure and k is the rate constant. Equation 3.4 is an integrated and rearranged version of Eyring's equation

$$\ln(k_o) = \left(\frac{\Delta V^\ddagger}{RT} \times P\right) + \ln(k_{P_o}) \quad (3.4)$$

where k_o is the rate constant, P is the specific pressure, and k_{P_o} is the rate constant at reference pressure P_o . This linearized form is used to calculate the ΔV^\ddagger from the slope of the plotted line.

In-Situ Activation Energy of Alcohol Oxidase

Arrhenius approach was used to determine the apparent activation energy, E_a , at 20.0 °C to 37 °C and 0.1 MPa. Figure 3.4 displays the linear relationship of the logarithm of the rate constant and the reciprocal of absolute temperature. An apparent E_a of $33.1 \pm 3.9 \text{ kJ mol}^{-1}$ with a correlation coefficient (R^2) 0.97 was determined by an *in-situ* determination of the apparent V_{\max} of AOX between 20.0 °C to 37 °C. The differences between 20.0 °C and 25.6 °C and between 25.6 °C and 31.4 °C were not significantly different as reported in Table 3.2. At 37 °C the V_{\max} , $4.6 \mu\text{M min}^{-1}$, was significantly greater than temperatures between 20.0 and 31.4 °C. Couderc and Baratti (1980) provided an E_a of 46.4 kJ mol^{-1} for AOX from *Pichia pastoris* between 10 °C to 37 °C. The difference between E_a from this study could be attributed to how activity was measured. Unfortunately, Couderc and Baratti (1980) did not make their methods clear when determining the effect of temperature on AOX. For this study the higher set point temperatures resulted in longer the come up time, which would have reduced the activity of AOX. Most likely Couderc and Baratti (1980) had all their reagents at the assay temperature and mixed them quickly before measuring the activity. In other words, there would have been no come up time to reduce the activity at any of the temperature set points, leading to a greater slope of the logarithm of rate constants *versus* the reciprocal absolute temperature. Kato et al. (1976) reported the E_a for AOX from *Candida boidinii* and *Hansenula polymorpha* to be slightly less than that of *Pichia pastoris* at 25 kJ mol^{-1} .

Activation Energy at High Pressure and High Temperature

The Arrhenius equation was also used to calculate the *in-situ* E_a for AOX at 0.1 MPa between 37 °C to 53.2 °C and 160 MPa between 37.0 °C to 53.2 °C (Figure 3.5). The apparent E_a

at 0.1 MPa was $8.5 \pm 15.52 \text{ kJ mol}^{-1}$ with a correlation coefficient of 0.092. The high standard error and low E_a at 0.1 MPa is explained by the temperature range 37 °C to 53.2 °C. The assumption would be that after 37 °C activation energy of activation would become activation energy of inactivation. Thus the V_{max} measurements after 37 °C to the high 40's would be in the transition stage where increased reaction rate and increasing rate of inactivation compete, producing a linear regression with slope near zero. In contrast, the apparent E_a at 160 MPa was $23.3 \pm 12.8 \text{ kJ mol}^{-1}$ with a correlation coefficient of 0.53. The E_a for AOX at 160 MPa between 37 °C to 53.2 °C is less than the E_a at 0.1 MPa between 20 °C to 37 °C lower temperatures, indicating that under high pressure AOX activity is less sensitive to changes in temperature.

Summary

At all temperatures between 37 °C and 53.2 °C, high pressure increased the catalytic rate of AOX as compared to the same temperatures at atmospheric pressure. A 3.2-fold increase in V_{max} occurred at 160 MPa at 53.2 °C as compared to the AOX activity at 37 °C and atmospheric pressure. At 160 MPa the optimum temperature for AOX shifted approximately 16.2 °C, as a result of the stabilizing effect of HHP. This study applied HHP and increased the activity of AOX at temperatures which thermally inactivate AOX at atmospheric pressure.

Table 3.1. *In-situ* V_{\max} for alcohol oxidase at 0.1 and 160 MPa determined by the rate of reaction for 1 min.

Temperature (°C)	V_{\max} ($\mu\text{M min}^{-1}$)					
	0.1 MPa		R^2	160 MPa		R^2
37.0	2.6 ^a	± 0.8	0.9992	4.5 ^a	± 1.6	0.9991
40.9	4.4 ^b	± 0.7	0.9996	7.2 ^{bc}	± 0.1	0.9997
44.9	2.8 ^a	± 0.5	0.9992	6.1 ^{ab}	± 1.3	0.9994
49.0	3.8 ^{ab}	± 0.5	0.9967	6.9 ^{abc}	± 0.4	0.9980
53.2	3.4 ^{ab}	± 0.4	0.9997	8.2 ^c	± 0.8	0.9997

^{a-d} Data are reported as the means ± standard deviation (n=3). Values with different letters within one column represent significant differences in V_{\max} ($\alpha=0.05$).

Table 3.2. *In-situ* V_{\max} for alcohol oxidase at 0.1 MPa between 20 to 37 °C.

Temperature (°C)	V_{\max} ($\mu\text{M min}^{-1}$)
20.0	2.1 ^a ± 0.4
25.6	3.0 ^{ab} ± 0.2
31.4	3.4 ^b ± 0.4
37.0	4.6 ^c ± 0.5

^{a-c} Data are reported as the means ± standard deviation (n=3). Values with different letters within one column represent significant differences in V_{\max} ($\alpha=0.05$).

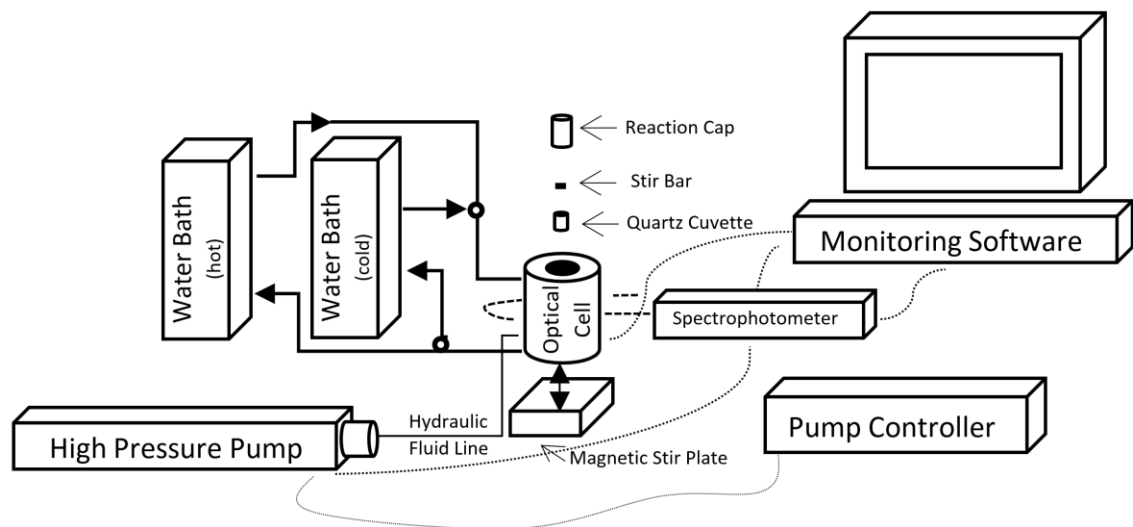


Figure 3.1. Schematic of high pressure processing equipment using an optical cell and spectrophotometer.

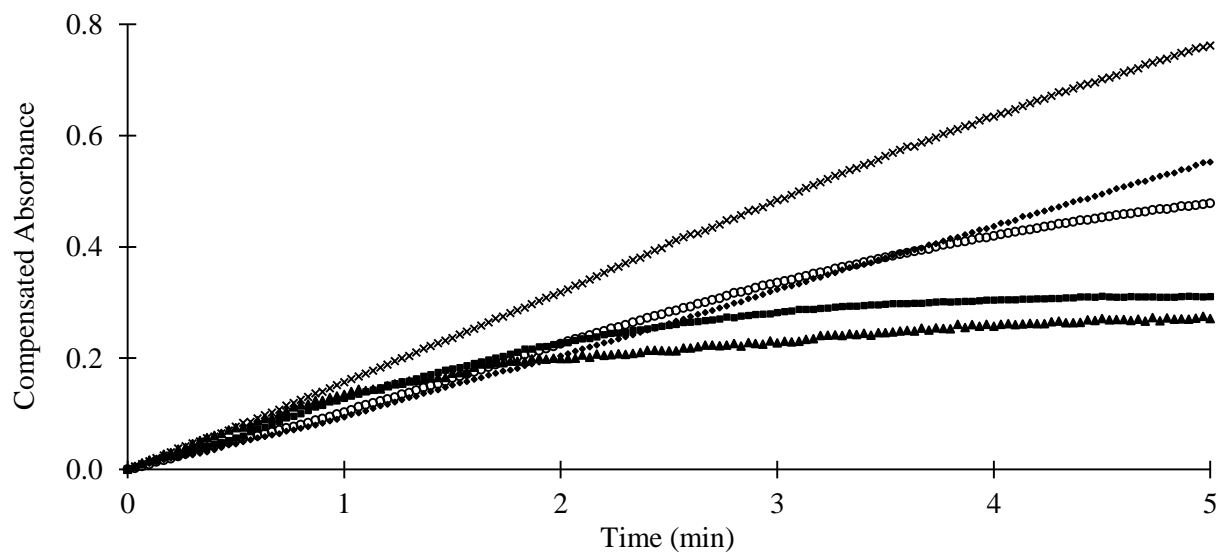


Figure 3.2. Activity displayed as change of absorbance for alcohol oxidase at 0.1 MPa and selected temperatures 37.0 (◆), 40.9 (x), 44.9 (○), 49.0 (■), 53.2 °C (▲).

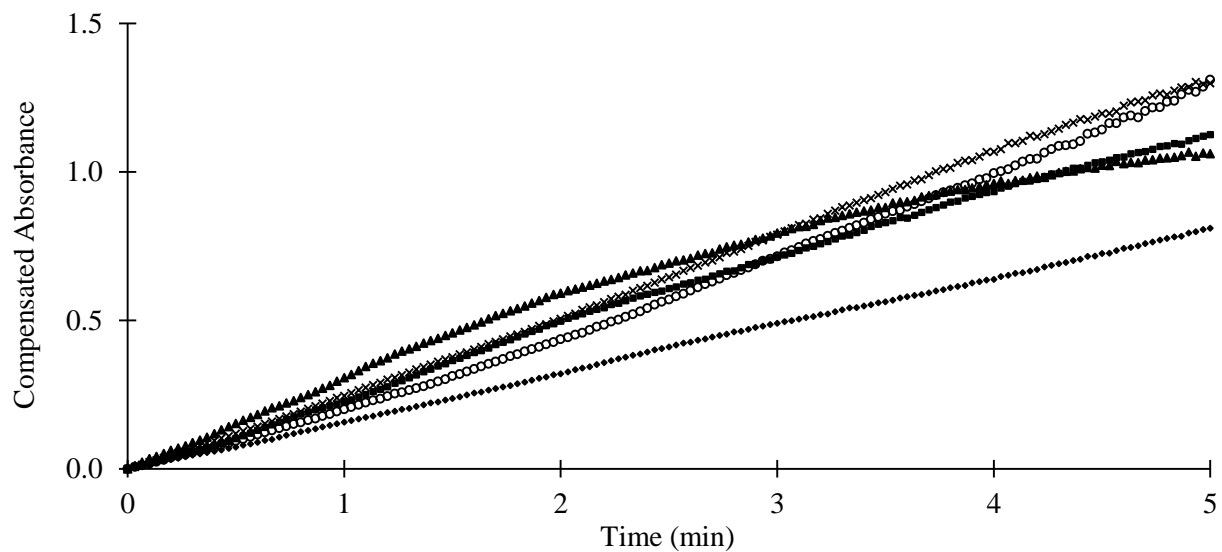


Figure 3.3. Activity displayed as change of absorbance for alcohol oxidase at 160 MPa and selected temperatures 37.0 (◆), 40.9 (x), 44.9 (○), 49.0 (■), 53.2 °C (▲).

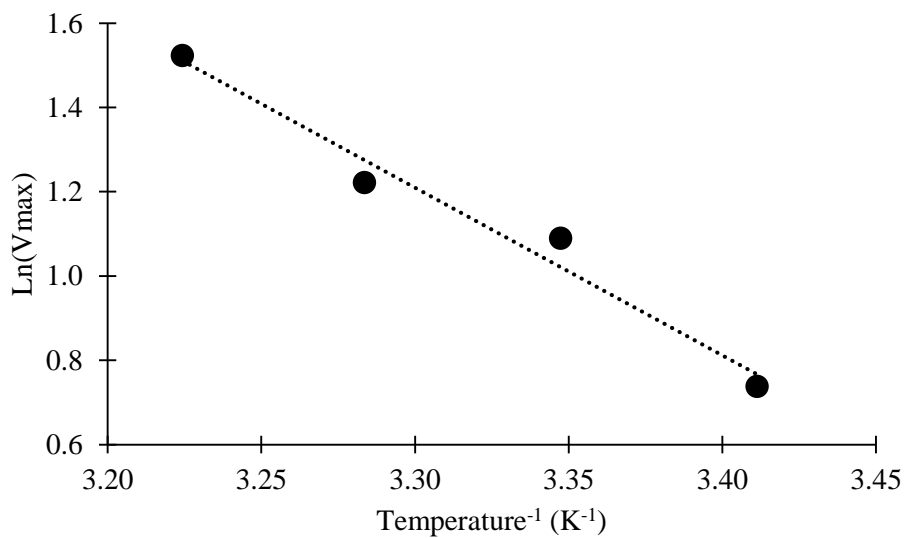


Figure 3.4. Arrhenius plot for activation energy of alcohol oxidase at 0.1 MPa (●) between 20 to 37 °C (displayed as 10^3 K).

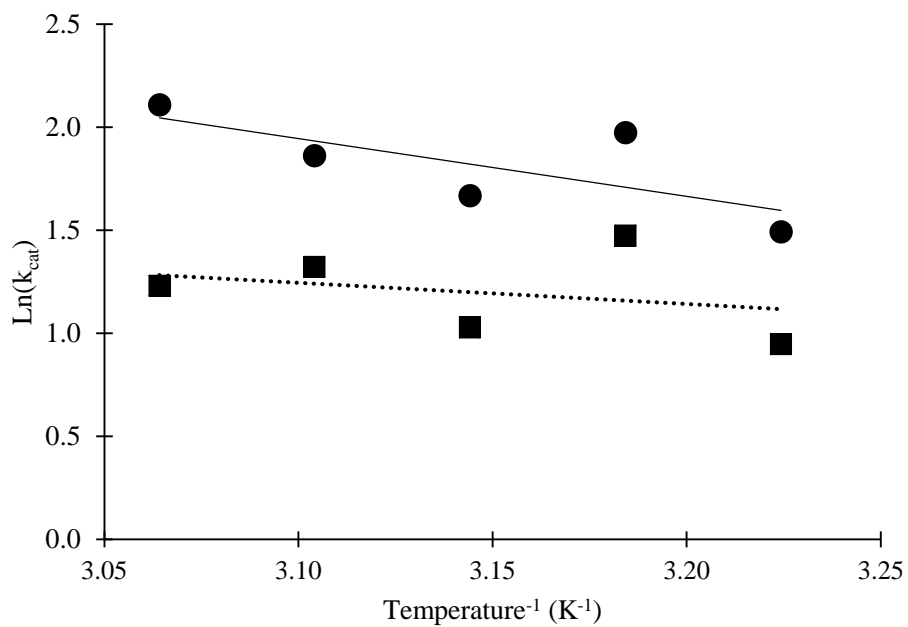


Figure 3.5. Arrhenius plot for AOX between 37 °C to 53.2 °C (displayed as 10^3 K) at 0.1 MPa (■) and 160 MPa (●).

CHAPTER 4

FINAL COMMENTS

Overview

In conclusion, HHP stabilized and increased the activity of AOX isolated from *Pichia pastoris*. Notably, pseudo-first order kinetics for the thermal inactivation of AOX at HHP and atmospheric pressure revealed two linear regions of inactivation when plotted as the logarithm of the residual activity *versus* time. The regions were described as an initial thermolabile region “L” where the enzyme inactivates rapidly and the second as a thermoresistant region “R” in which a second fraction of active AOX is more stable. Slowest rates of inactivation were observed between 40 MPa to 200 MPa, in particular between 120 MPa and 160 MPa. Transition from stabilization to destabilization occurred at pressures greater than 160 MPa. A purified enzyme was used thus we hypothesize that the homooctameric structure of AOX dissociates into active subunits that are stabilized by pressure.

A temperature-controlled HHP optical cell was used to spectrophotometrically determine the activity, *in-situ*, of AOX. At all temperatures between 37 °C to 59.1 °C, the high pressure of 160 MPa increased the catalytic rate of AOX as compared to the same temperature at atmospheric pressure. Compared to the optimal temperature of 37 °C, at atmospheric pressure, AOX activity increased 2.8 times at 160 MPa and 55.8 °C. High hydrostatic pressure processing is a relevant tool for the optimization of AOX, in terms of both stability and activity.

Future Work

Utilization of the optimum pressure range (120 MPa to 160 MPa) for AOX stabilization against thermal inactivation can be a resource for the development of alcohol biosensors at HHP. Also, the discovery of the thermolabile and thermoresistant regions of inactivation should be accounted for when developing the alcohol biosensor. For example, because it is known that the thermoresistant fraction of AOX is more stable to thermal inactivation, AOX should be processed to remove the thermolabile fraction, then the thermoresistant fraction be immobilized to the working electrode. A future hurdle to overcome is the immobilization of the stabilized conformation of AOX onto the working electrode. The most likely situation would be to build the biosensor in the reactor under pressure.

Further investigation is needed to determine why AOX has two regions of thermal inactivation. Due to the multimeric nature of AOX it would be beneficial to know if the enzyme dissociates into stable intermediates and if so the size of such intermediates. As Trovaslet et al. (2003) stated it is known that HHP modifies the structure of enzymes by altering intra- and intermolecular interactions that effect protein stability, yet, minimal studies have attempted to correlate the conformational changes to catalytic activity. Native polyacrylamide gel electrophoresis (PAGE) was performed to determine if AOX dissociates into stable subunits (monomers, dimers, trimers, etc.).

Unfortunately, the enzyme concentration was too low for visualization of the bands, Even though enzyme concentration was greatly increased, 14.3-fold, as compared to the enzyme concentration used for treatment of the R fraction (1.5 unit mL^{-1}) in Chapter 2. Interestingly, the plastic pouch with the high enzyme concentration was clear before treatment but became turbid after pressure-temperature treatments, indicating aggregation, even though the sample exhibited

activity. The treatments were at 59.1 °C at atmospheric pressure and 160 MPa. The processing times for 0.1 MPa was 0 and 0.5 min with resulting activities of 0.473 and 0.214 unit mg⁻¹ AOX, respectively. The processing time for 160 MPa was 4 and 16 min with resulting activities of 1.390 and 1.029 unit mg⁻¹ AOX, respectively. All four treatments resulted in a cloudy post treatment pouch. It would be interesting to separate the aggregates from solution and examine the activity of both after varying pressure-temperature-process time combinations. Potentially, this could be a method to separate the thermolabile fraction of AOX from the thermoresistant fraction. As a result of the high enzyme concentration needed for Native PAGE to work, the Western Blot technique was suggested, which uses a lower enzyme concentration to visualize the effect HHP is having on AOX subunits.

Experimental design adjustments to Chapter 3's study on the effect of HHP on the catalytic rate of AOX should be made. Then the experiment should be repeated with the alterations to obtain more reliable data. Adjustments would include higher AOX concentration, a lower temperature range (37 to 55 °C), analysis of absorbance change during come up time as well as increase in length of reaction recording time once set points are reached, more frequent data collection, and increased substrate concentration.

Although the result of Chapter 3's study on the effects of HHP on catalytic rate of AOX had high experimental error, a conclusion can be made that HHP increased the V_{max} of AOX with the substrate methanol. Future work should be performed to determine if HHP can also increase the catalytic rate of AOX of substrates which produce valuable chemicals. Individual studies must be performed to determine the optimal environment, including pressure,

temperature, pH and solvent that produces the greatest increase on AOX activity for each substrate.

REFERENCES

- Abayomi, L.A., Terry, L.A., White, S.F., Warner, P.J., (2006). Development of a disposable pyruvate biosensor to determine pungency in onions (*Allium cepa* L.). *Biosensors and Bioelectronics* 21(11), 2176-2179.
- Akin, M., Yuksel, M., Geyik, C., Odaci, D., Bluma, A., Hoepfner, T., Beutel, S., Scheper, T., Timur, S., (2010). Alcohol biosensing by polyamidoamine (PAMAM)/cysteamine/alcohol oxidase-modified gold electrode. *Biotechnology Progress* 26(3), 896-906.
- AOAC, (2012). *Official Methods of Analysis* (19 ed). Association of Official Analytical Chemists, Gaithersburg, MD.
- Aymard, C., Belarbi, A., (2000). Kinetics of thermal deactivation of enzymes: A simple three parameters phenomenological model can describe the decay of enzyme activity, irrespectively of the mechanism. *Enzyme and Microbial Technology* 27(8), 612-618.
- Azevedo, A.M., Cabral, J.M.S., Gibson, T.D., Fonseca, L.P., (2004a). Operation and performance of analytical packed-bed reactors with an immobilised alcohol oxidase. *Journal of Molecular Catalysis B: Enzymatic* 28(2-3), 45-53.
- Azevedo, A.M., Cabral, J.M.S., Prazeres, D.M.F., Gibson, T.D., Fonseca, L.P., (2004b). Thermal and operational stabilities of *Hansenula polymorpha* alcohol oxidase. *Journal of Molecular Catalysis B: Enzymatic* 27(1), 37-45.
- Azevedo, A.M., Prazeres, D.M., Cabral, J.M., Fonseca, L.P., (2005). Ethanol biosensors based on alcohol oxidase. *Biosensors and Bioelectronics* 21(2), 235-247.
- BACtrack, (2016). Bactrack® wins “Wearable alcohol biosensor challenge” issued through National Institutes of Health (NIH).
- Balny, C., Masson, P., Heremans, K., (2002). High pressure effects on biological macromolecules: From structural changes to alteration of cellular processes. *Biochimica et Biophysica Acta (BBA) - Protein Structure and Molecular Enzymology* 1595(1–2), 3-10.
- Barsan, M.M., Brett, C.M.A., (2008). An alcohol oxidase biosensor using PNR redox mediator at carbon film electrodes. *Talanta* 74(5), 1505-1510.
- Betancor, L., Hidalgo, A., Fernandez-Lorente, G., Mateo, C., Fernandez-Lafuente, R., Guisan, J.M., (2003). Preparation of a stable biocatalyst of bovine liver catalase using immobilization and postimmobilization techniques. *Biotechnology Progress* 19(3), 763-767.

- Bilbao-Sáinz, C., Younce, F.L., Rasco, B., Clark, S., (2009). Protease stability in bovine milk under combined thermal-high hydrostatic pressure treatment. *Innovative Food Science & Emerging Technologies* 10(3), 314-320.
- Boonyaratanakornkit, B.B., Park, C.B., Clark, D.S., (2002). Pressure effects on intra- and intermolecular interactions within proteins. *Biochimica et Biophysica Acta (BBA) - Protein Structure and Molecular Enzymology* 1595(1–2), 235-249.
- Boujtita, M., Hart, J.P., Pittson, R., (2000). Development of a disposable ethanol biosensor based on a chemically modified screen-printed electrode coated with alcohol oxidase for the analysis of beer. *Biosensors and Bioelectronics* 15(5-6), 257-263.
- Bridgman, P., (1914). The coagulation of albumen by pressure. *Journal of Biological Chemistry* 19(4), 511-512.
- Buckow, R., Weiss, U., Knorr, D., (2009). Inactivation kinetics of apple polyphenol oxidase in different pressure-temperature domains. *Innovative Food Science & Emerging Technologies* 10(4), 441-448.
- Bucur, B., Radu, G., Toader, C., (2008). Analysis of methanol–ethanol mixtures from falsified beverages using a dual biosensors amperometric system based on alcohol dehydrogenase and alcohol oxidase. *European Food Research and Technology* 226(6), 1335-1342.
- Chinnadayyala, S.R., Kakoti, A., Santhosh, M., Goswami, P., (2014). A novel amperometric alcohol biosensor developed in a 3rd generation bioelectrode platform using peroxidase coupled ferrocene activated alcohol oxidase as biorecognition system. *Biosensors and Bioelectronics* 55, 120-126.
- Chinnadayyala, S.R., Santhosh, M., Singh, N.K., Goswami, P., (2015). Alcohol oxidase protein mediated *in-situ* synthesized and stabilized gold nanoparticles for developing amperometric alcohol biosensor. *Biosensors and Bioelectronics* 69, 155-161.
- Couderc, R., Baratti, J., (1980). Oxidation of methanol by the yeast, *Pichia pastoris*. Purification and properties of the alcohol oxidase. *Agricultural and Biological Chemistry* 44(10), 2279-2289.
- Dallet, S., Legoy, M.D., (1996). Hydrostatic pressure induces conformational and catalytic changes on two alcohol dehydrogenases but no oligomeric dissociation. *Biochimica Et Biophysica Acta-Protein Structure and Molecular Enzymology* 1294(1), 15-24.
- Dalmadi, I., Rapeanu, G., Van Loey, A., Smout, C., Hendrickx, M., (2006). Characterization and inactivation by thermal and pressure processing of strawberry (*Fragaria ananassa*) polyphenol oxidase: A kinetic Study. *Journal of Food Biochemistry* 30(1), 56-76.
- Dienys, G., Jarmalavicius, S., Budrien, S., Citavičius, D., Sereikait, J., (2003). Alcohol oxidase from the yeast *Pichia pastoris*—a potential catalyst for organic synthesis. *Journal of Molecular Catalysis B: Enzymatic* 21(1–2), 47-49.

- Duff, S.J.B., Murray, W.D., (1988). Comparison of free and immobilized *Pichia pastoris* cells for conversion of ethanol to acetaldehyde. *Biotechnology and Bioengineering* 31(8), 790-795.
- Duff, S.J.B., Murray, W.D., (1989). Oxidation of benzyl alcohol by whole cells of *Pichia pastoris* and by alcohol oxidase in aqueous and nonaqueous reaction media *Biotechnology and Bioengineering* 34(2), 153-159.
- Eisenmenger, M.J., Reyes-De-Corcuera, J.I., (2009a). High hydrostatic pressure increased stability and activity of immobilized lipase in hexane. *Enzyme and Microbial Technology* 45(2), 118-125.
- Eisenmenger, M.J., Reyes-De-Corcuera, J.I., (2009b). High pressure enhancement of enzymes: A review. *Enzyme and Microbial Technology* 45(5), 331-347.
- Evers, M.E., Harder, W., Veenhuis, M., (1995). *In vitro* dissociation and re-assembly of peroxisomal alcohol oxidases of *Hansenula polymorpha* and *Pichia pastoris*. *FEBS Letters* 368(2), 293-296.
- Fujii, T., Tonomura, K., (1972). Oxidation of methanol, formaldehyde and formate by a *Candida* species. *Agricultural and Biological Chemistry* 36(13), 2297-2306.
- Garcia-Palazon, A., Suthanthangjai, W., Kajda, P., Zabetakis, I., (2004). The effects of high hydrostatic pressure on *beta*-glucosidase, peroxidase and polyphenoloxidase in red raspberry (*Rubus idaeus*) and strawberry (*Fragaria x ananassa*). *Food Chemistry* 88(1), 7-10.
- Gianfreda, L., Marrucci, G., Grizzuti, N., Greco, G., (1984). Acid-phosphatase deactivation by a series mechanism. *Biotechnology and Bioengineering* 26(5), 518-527.
- Gibson, T.D., Hulbert, J.N., Woodward, J.R., (1993). Preservation of shelf-life of enzyme-based analytical systems using a combination of sugars, sugar alcohols and cationic polymers of zinc ions. *Analytica Chimica Acta* 279(1), 185-192.
- Goodman, J.M., Scott, C.W., Donahue, P.N., Atherton, J.P., (1984). Alcohol oxidase assembles post-translationally into the peroxisome of *Candida boidinii*. *Journal of Biological Chemistry* 259(13), 8485-8493.
- Goodrich, R.M., Braddock, R.J., Parish, M.E., Sims, C.A., (1998). Bioconversion of citrus aroma compounds by *Pichia pastoris*. *Journal of Food Science* 63(3), 445-449.
- Goriushkina, T.B., Soldatkin, A.P., Dzyadevych, S.V., (2009). Application of amperometric enzyme biosensors for Wine and must Analysis. *Procedia Chemistry* 1(1), 277-280.
- Greco, G., Gianfreda, L., (1984). An experimental-technique for the discrimination between series and parallel mechanisms of enzyme deactivation. *Biotechnology Letters* 6(11), 693-697.

- Gruskiene, R., Kairys, V., Matijosyte, I., (2015). Clea-based immobilization of methylotropic yeast alcohol oxidase: Influence on storage stability and reaction efficiency. *Organic Process Research & Development* 19(12), 2025-2033.
- Hawley, S.A., (1971). Reversible pressure-temperature denaturation of chymotrypsinogen. *Biochemistry* 10(13), 2436.
- Hendrickx, M., Ludikhuyze, L., Van den Broeck, I., Weemaes, C., (1998). Effects of high pressure on enzymes related to food quality. *Trends in Food Science & Technology* 9(5), 197-203.
- Isobe, K., Kataoka, M., Ogawa, J., Hasegawa, J., Shimizu, S., (2012). Microbial oxidases catalyzing conversion of glycolaldehyde into glyoxal. *New Biotechnology* 29(2), 177-182.
- Isobe, K., Kato, A., Sasaki, Y., Suzuki, S., Kataoka, M., Ogawa, J., Iwasaki, A., Hasegawa, J., Shirnizu, S., (2007). Purification and characterization of a novel alcohol oxidase from *Paenibacillus* sp AIU 311. *Journal of Bioscience and Bioengineering* 104(2), 124-128.
- Isobe, K., Nishise, H., (1995). A new enzymatic method for glycolaldehyde production from ethylene glycol. *Journal of Molecular Catalysis B-Enzymatic* 1(1), 37-43.
- Janssen, F.W., Ruelius, H.W., (1968). Alcohol oxidase, a flavoprotein from several basidiomycetes species. *Biochimica et Biophysica Acta (BBA) - Enzymology* 151(2), 330-342.
- Kamanin, S.S., Arlyapov, V.A., Machulin, A.V., Alferov, V.A., Reshetilov, A.N., (2015). Biosensors based on modified screen-printed enzyme electrodes for monitoring of fermentation processes. *Russian Journal of Applied Chemistry* 88(3), 463-472.
- Katchalski-Katzir, E., (1993). Immobilized enzymes — learning from past successes and failures. *Trends in Biotechnology* 11(11), 471-478.
- Kato, N., Omori, Y., Tani, Y., Ogata, K., (1976). Alcohol oxidases of *Kloeckera* sp and *Hansenula polymorpha* - catalytic properties and subunit structures. *European Journal of Biochemistry* 64(2), 341-350.
- Keesey, J., (1987). *Biochemica information: A revised biochemical reference source*. Boehringer Mannheim Biochemicals.
- Kiralp, S., Topcu, A., Bayramoglu, G., Arica, M.Y., Toppare, L., (2008). Alcohol determination via covalent enzyme immobilization on magnetic beads. *Sensors and Actuators B-Chemical* 128(2), 521-528.
- Kuswandi, B., Irmawati, T., Hidayat, M.A., Jayus, Ahmad, M., (2014). A simple visual ethanol biosensor based on alcohol oxidase immobilized onto polyaniline film for halal verification of fermented beverage samples. *Sensors* 14(2), 2135-2149.

- Limtong, S., Srisuk, N., Yongmanitchai, W., Yurimoto, H., Nakase, T., (2008). *Ogataea chonburiensis* sp nov and *Ogataea nakhonphanomensis* sp nov., thermotolerant, methylotrophic yeast species isolated in thailand, and transfer of *Pichia siamensis* and *Pichia thermomethanolica* to the genus *Ogataea*. International Journal of Systematic and Evolutionary Microbiology 58, 302-307.
- Lopez-Gallego, F., Betancor, L., Hidalgo, A., Dellamora-Ortiz, G., Mateo, C., Fernández-Lafuente, R., Guisán, J.M., (2007). Stabilization of different alcohol oxidases via immobilization and post immobilization techniques. Enzyme and Microbial Technology 40(2), 278-284.
- Majerski, P.A., Piskorz, J.K., Radlein, D.S.A.G., (2006). Production of glycolaldehyde by hydrous thermolysis of sugars - us7094932 B2, *Official Gazette of the United States Patent and Trademark Office Patents*.
- Mello, L.D., Kubota, L.T., (2002). Review of the use of biosensors as analytical tools in the food and drink industries. Food Chemistry 77(2), 237-256.
- Michels, P.C., Clark, D.S., (1997). Pressure-enhanced activity and stability of a hyperthermophilic protease from a deep-sea methanogen. Applied and Environmental Microbiology 63(10), 3985-3991.
- Mozhaev, V.V., Lange, R., Kudryashova, E.V., Balny, C., (1996). Application of high hydrostatic pressure for increasing activity and stability of enzymes. Biotechnology and Bioengineering 52(2), 320-331.
- Murray, W.D., Duff, S.J.B., (1990). Biooxidation of aliphatic and aromatic high molecular weight alcohols by *Pichia pastoris* alcohol oxidase Applied Microbiology and Biotechnology 33(2), 202-205.
- Nunes, W.d.S., de Oliveira, C.S., Alcantara, G.B., (2016). Ethanol determination in frozen fruit pulps: An application of quantitative nuclear magnetic resonance. Magnetic Resonance in Chemistry 54(4), 334-340.
- Ough, C.S., Amerine, M.A., (1988). *Methods for Analysis of Musts and Wines* (2 ed). John Wiley & Sons, Inc., NY, USA.
- Park, J.-K., Yee, H.-J., Lee, K.S., Lee, W.-Y., Shin, M.-C., Kim, T.-H., Kim, S.-R., (1999). Determination of breath alcohol using a differential-type amperometric biosensor based on alcohol dehydrogenase. Analytica Chimica Acta 390(1-3), 83-91.
- Patel, N.G., Meier, S., Cammann, K., Chemnitus, G.C., (2001). Screen-printed biosensors using different alcohol oxidases. Sensors and Actuators B: Chemical 75(1-2), 101-110.
- Patel, R.N., Hou, C.T., Laskin, A.I., Derelanko, P., (1981). Microbial oxidation of methanol - properties of crystallized alcohol oxidase from a yease, *Pichia* sp. Archives of Biochemistry and Biophysics 210(2), 481-488.

- Personna, Y.R., Slater, L., Ntarlagiannis, D., Werkema, D., Szabo, Z., (2013). Electrical signatures of ethanol–liquid mixtures: Implications for monitoring biofuels migration in the subsurface. *Journal of Contaminant Hydrology* 144(1), 99-107.
- Pinnacle, T.I., (2012). *Biosensors*, Lawrence, KS.
- Pundir, C.S., Devi, R., (2014). Biosensing methods for xanthine determination: A review. *Enzyme and Microbial Technology* 57, 55-62.
- Reyes-De-Corcuera, J.I., (2015). Electrochemical biosensors, *Encyclopedia of Agricultural, Food, and Biological Engineering*, 2 ed. CRC Press, Boca Raton
- Terefe, N.S., Yang, Y.H., Knoerzer, K., Buckow, R., Versteeg, C., (2010). High pressure and thermal inactivation kinetics of polyphenol oxidase and peroxidase in strawberry puree. *Innovative Food Science & Emerging Technologies* 11(1), 52-60.
- Terry, L.A., White, S.F., Tigwell, L.J., (2005). The application of biosensors to fresh produce and the wider Food industry. *Journal of Agricultural and Food Chemistry* 53(5), 1309-1316.
- Tomasi, D., Gaiotti, F., Jones, G.V., (2013). *The Power of the Terroir : The Case Study of Prosecco Wine*. Springer, Basel ; New York
- Tomlin, B.D., Jones, S.E., Reyes-De-Corcuera, J.I., (2013). High hydrostatic pressure protection of a pectinase cocktail against thermal inactivation. *Journal of Food Engineering* 116(3), 674-680.
- Tomlin, B.D., Jones, S.E., Teixeira, A.A., Correll, M.J., Reyes-De-Corcuera, J.I., (2014). Kinetics of viscosity reduction of pectin solutions using a pectinase formulation at high hydrostatic pressure. *Journal of Food Engineering* 129, 47-52.
- Trovaslet, M., Dallet-Choisy, S., Meersman, F., Heremans, K., Balny, C., Legoy, M.D., (2003). Fluorescence and ftir study of pressure-induced structural modifications of horse liver alcohol dehydrogenase (HLADH). *European Journal of Biochemistry* 270(1), 119-128.
- Trovaslet, M., Legoy, M.D., Dallet-Choisy, S., (2004). Effects of hydrostatic pressure on horse liver alcohol dehydrogenase (HLADH): A new way of analyzing kinetic study. *Cellular and Molecular Biology* 50(4), 353-359.
- Ukeda, H., Ishii, T., Sawamura, M., Isobe, K., (1998). Glycolaldehyde production from ethylene glycol with immobilized alcohol oxidase and catalase. *Bioscience Biotechnology and Biochemistry* 62(8), 1589-1591.
- Weemaes, C.A., Ludikhuyze, L.R., Van den Broeck, I., Hendrickx, M.E., (1998). Kinetics of combined pressure-temperature inactivation of avocado polyphenoloxidase. *Biotechnology and Bioengineering* 60(3), 292-300.

Wen, G., Zhang, Y., Shuang, S., Dong, C., Choi, M.M.F., (2007). Application of a biosensor for monitoring of ethanol. *Biosensors and Bioelectronics* 23(1), 121-129.

Wu, X.J., Choi, M.M.F., Chen, C.S., Wu, X.M., (2007). On-line monitoring of methanol in n-hexane by an organic-phase alcohol biosensor. *Biosensors and Bioelectronics* 22(7), 1337-1344.

Xylem, I., (2015). Ysi 2900 series biochemistry analyzers: Operations and maintenance manual.

Yablotskii, K.V., Shekhovtsova, T.N., (2010). Enzymatic determination of anions. *Journal of Analytical Chemistry* 65(7), 660-673.

Zhao, L., Liu, Q., Yan, S., Chen, Z., Chen, J., Li, X., (2013). Multimeric immobilization of alcohol oxidase on electrospun fibers for valid tests of alcoholic saliva. *Journal of Biotechnology* 168(1), 46-54.